上海海洋大学

2022 年工程学院

大学生创新创业成果汇编

2023 年 7 月

目　录

一、大学生创新项目

1. 大学生创新项目统计表

2022 年大学生校级项目

项目名称	项目负责人姓名	项目负责人专业/学号	项目其他成员信息	指导老师姓名
自主飞行剪枝无人机研究实施	和远航	2027120/电气	2027124/凡兴波 2027121/申晓磊 2015421/董君禹	张增敏
“长江口”中大型鱼类 3D 仿真及 AI 识别实验	哈国杨	2022407/机制	2022423/向豪 1953121/杨进龙 1913321/滕飞 2013310/程子绮	张莉君
基于物联网的智能花卉养护系统	陈长	1927228/电气	1927221/张文峰 2027103/卢梁羽骐	高玉娜
基于 TIVA 的无人机自动充电系统设计	何施呈	2027114/电气	2130315/马运强 2126516/唐智圆 2126522/熊昊 2126508/乔奕玮	曹莉凌
多功能无人机与无人船协同控制系统	武俊岑	2022107/机制	1929135/王召熙 1953218/陶翔 1933108/朱耘颖	刘雨青
基于四旋翼的对水质水面检测	吴涵	2027203/电气	2027227/朱春炼 2027110/朱昊 2126101/刘彦男	高玉娜
老幼出行多功能一体化便携小车设计	韩亮	2025125/工业	2130201/陈一卓 2130207/张明腾 2025103/蔡苗苗 2025118/鲁彪	姜波
无人船水质检测与数据传输存储系统设计	鲍哲晟	2027119/电气	2027111/黄嘉隽 2022107/武俊岑 2022128/王浩然 2126211/沈翰廷	刘雨青
基于声学的南美白对虾生物行为研究	刘岩青	2025208/工业	2025217/陈慕尧 2025219/李东霖 2052633/宋卓 2052639/谯伟豪	吴迪

智能测温消毒镜	甄世召	2025215/工业	2025216/崔栋凯 2025107/彭韵桐 2025108/许娜娜	吕超
鱼贝类外形尺寸及重量自动化检测样机	朱楚亮	2022119/机制	2011410/吕天翊 2052528/赵浩杰	张俊
高校共享单车投放系统改进	赵布衣	2028105/物工	2028106/陈菲洋 2028104/张思琪 2028205/方书颖	陶宁蓉
自动捆扎机设计及运用	李开拓	2025218/工业	2069214/梁丽敏 2025217/陈慕尧 2025221/张馨	吴迪
仿生鱼的减阻机理分析	柯政帆	2130719/制造	2126507/仲泽晨 2126224/买文杰 2126225/韩东兴 2130127/李琛	陈雷雷
基于无线充电技术和物联网的仿生海龟群研究与实现	华奕龙	2027228/电气	2027129/秦翰轩 2126203/黄旻钰 2126503/李奕蓉 2126219/郭继凯	谢嘉
面向用户行为能力分析的智能衣架研究	李路阳	1927109/电气	1927117/陆嘉波 1927124/王韶洋 2022125/黄森 2126216/宋嘉晨	杨琛
一种废玻璃瓶回收装置的设计	周琪	1925116/工业	1925111/朱梦祥	张丽珍
水面水下两用小型救援航行器	张涛涛	2022417/机制	2022407/哈国杨 2029208/曾诗琪 2021107/徐子沐	张俊
自动化脱贝清洗装置的研制	姚宇	2022428 机制	2022417/张涛涛 2022415/姜项豪	田中旭
小丑鱼号——鹿角珊瑚种植 ROV	张瑞宇	2022307/机制	2130219/卢致任 1921217/王维捷 1941111/李匡	张丽珍

河蟹蟹身分离装置设计	徐杰	1922414/机制	2023126/罗森林 2023114/冯骏 2022322/秦庆华 2022308/唐崇策	赵煜
基于四旋翼的果实巡检及无人采摘系统的设计	徐信	2027201/电气	2022101/苑晓聪 2027202/张雅韵 1827108/王屹林 2028211/曹怡然	曹莉凌
采光顶智能遮阳帘	袁旭	1922317/机制	1922326/袁东迎	吴子岳
基于 autolabor 小车的移动口罩识别装置	王鑫涛	1923117/测控	1923116/徐吉 1923119/吴帅 1923125/李晋生	董兆鹏
基于区块链技术的 web3.0 时代去中心化的社交软件	吴宇恒	2025117/工业	1911726/张钦义 2052543/赵坤 2052545/恰拉帕提·我鲁曼 1953123/刘定邦	魏立斐
一种便携式乒乓球自动发球机	杨林	2041131/机械	1922409/佘云龙 2022410/任岳 1932426/孟思杰	袁军亭
一种用于渔业资源增殖放流的装置	刘健磊	2022211/机制	1925111/朱梦祥 1925116/周琪	张丽珍
带隔音装置的简易水果成熟度仪	莫维文	2126326/控制	2126318/陶宏宇 2126324/仝世锦 2023125/程谦毅 1922311/范智超	赵煜
“邻里同行”私家车共享平台	秦杰浚	1925216/工业	1927219/胡鑫宝 2028225/郭耀泽 2060217/梁展鹏 2152205/郑琳凡	姜波
智能控制便携式风扇	郎维荣	2025122/工业	2025121/张鑫 2025123/冯昌林	上官春霞
光伏电站无人机巡检系统	张雅韵	2027202/电气	2027203/吴涵 2126101/刘彦男	曹莉凌

自适应 3D 打印机的设计	袁毅涛	1927207/电气	1927221/张文峰 1927216/高凯文 1927218/洪健	吴清云
一种环境保护用水样采集分析装置	赵博涵	2022427/机制	2027122/巴文杰 2022219/王宸烨	刘雨青
清水蟹养殖场无人机投喂作业路径规划	李京昊	1925124/工业	1925118/向希尧 1925107/亚库普·麦提图尔荪 2025121/张鑫 2025122/郎维荣	上官春霞

2022 年大学生市级项目

项目名称	项目负责人姓名	项目负责人专业/学号	项目其他成员信息	指导老师姓名
一种用于滩涂养殖贝类采集与分拣的智能化样机研发	付文森	工业/2025209	康明娣/2025209、闵佳婧/2011413、李盼盼/2029512、王若/2041108	张俊
一种智能安全帽设计	曾瑞琪	工业/2025207	凌小婵/2025201、郭晗潇/2025202、徐怡萍/2025203、朱哲慧/2025205	陈成明
基于智能机械臂的水产品分拣装置	姜龙	测控/2023124	凌宇星/2023118、王速点/2011612、韩煜航/2126308	李俊
基于 IOT 物联网技术的环保污染治理配电终端研究	胡彦	电气/2027211	胡涵博/2027221、王振楠/2126512	匡兴红、霍海波
便携消防水带自动收纳机	刘俊辰	工业/2025214	殷之抗/2025213、贾春旺/2025212、付文森/2025209	张丽珍
智能窗户	康明娣	机制/2022303	殷之抗/2025213、徐怡萍/2025203、覃夏楠/2042226	高丽
一种老年人智能预警及	刘世功	工业/2025112	刘岩青/2025208、曾瑞琪/2025207、陈冉	陈成明、李志坚

防摔装置			/2052411、孙炳颜 /2130117	
基于雾化饵料投喂的立体监控养殖智能化水下航行器	李东霖	工业 /2025219	李佳明/2041112、滕博 /2130107、袁瑞 2130216	陈成明、上官春霞
基于 AI 识别的防疫智能巡检机器人	梁康	测控 /2023130	贾超/2023123、林国睿 /2023128、吴正泓 /2023127、冯向鑫 /2023129	张铮
“中国魔方”——基于 TRIZ 理论的沙障铺设小车	杨尚青	机制 /1922221	施冬凡/1922211、汪子杰/1922217	胡庆松
长条形鱼类自动化整理装置开发	王奕桐	制造 /2130101	王润泽 2130108	田中旭
智能助老无人药盒	姜子昂	电气 /1922407	陈子轩/2027223、李扬濛/2027209、卢祥 /2028220	刘雨青
无人机病虫害预防与识别	王孝东	物工 /1928121	李科琪/1928128、苏康 /1928126、胡聪 /1928122、秦昊泓 /1928125	梁贺君
基于手机 APP 实时计费的景区智能跟人小车创业计划研究实施	徐伟钤	电气 /2027115	杨鑫宇/2015312、谢誉坤/2092330、邱玥 /2027101、王彩霞 /2126504	谢嘉
基于北斗系统的多功能示位器	吴扬	测控 /2023115	胡涵/2052607、黄宇庆 /1953127、麦富城 /1823129、陈丹伟 /2023119	张铮
一种水产养殖用浮漂垃圾收集与自动投喂智能机器人	苑晓聪	机制 /2022101	王子宸/2021212、徐信 /2027201、蒙宣谕 /2028224、刘春雨 /2022102	崔秀芳

扫把粘连物清洁装置	崔栋凯	工业/2025216	甄世召/2025215、许娜娜/2025108、杜媛媛/2028207	吕超
电动无尘黑板擦	潘金铎	控制/2126124	胡治伟/2092450、洪弘/2144109、吴俊逸/2130211	杨琛
无人测温小车	陆智裕	机制/1922412	曹煜希/1922411、周俊似/1922422、顾鑫晖/1922413	吴子岳
双向储能变流器 PCS 系统的设计	路军	电气/1927229	赵烨/2027206、安云峰/2027128、蔡承儒/2126206、倪榕键 2126218	金光哲
基于自动智能地锁的共享云平台系统	陈天野	机制/1922121	徐文静/1940114、龚子涵/1922110	王斌
电控液压水下智能网板的研究及设计	褚骏豪	控制/2126421	胡澳宾/2022418、强冉/2126214、程振峰/2021233、张海波/2130416	李俊、孔祥洪

2.优秀案例

一种水产养殖用浮漂垃圾收集与自动投喂智能机器人

案例摘要

随着水产养殖种类的不断增多以及养殖环境与养殖方式的不断转变，水产养殖行业产生的经济效益逐年攀升，并仍存在巨大商业潜力。然而，对于迫切追求扩大生产的局面，传统的饵料投喂技术极大损耗人力物力，已经不能满足现代水产养殖的需求，而饵料投喂技术是养殖主生产过程中重要环节，直接影响着养殖品种的产量和质量的提升。

本项目在投饵装置上进行改进，提出一种自动收集漂浮垃圾的水产养殖用浮漂垃圾收集与自动投喂智能机器人，实现自动收集漂浮垃圾、自动投饵，解放人力，同时极大保障了水产生物的营养供给及水体环境维护。我国目前的养殖模式和养殖环境决定了还不能应用先进的智能投饲系统。许多小型养殖户在鱼塘中还是只能使用小型的电力自动投饵机。而在海洋牧场中，尤其是在远离海岸的养殖区，没有电力供应，养殖户依然采用人工投喂，如果遇到风浪或阴雨天，投喂难度成倍增加，既威胁养殖户人身安全又影响投喂效果，降低了收益。对此，自动投饵机在未来的首要发展方向为具备一定可靠性的清洁能源投饵机。针对这一现状，本项目致力研发一种体积小、灵活性高、清洁环保且适用范围广的自动投饵装置，为渔业养殖饵料投喂提供新的思路，对传统水产养殖注入新的科技力量。

（一）项目的选题、目的与意义

习近平总书记曾强调，坚持把解决好“三农”问题作为全党工作重中之重，而智慧农业是农业的根本出路，中央一号文件也连续多年发布与智慧农业相关政策。目前，全球都在加快智慧农业发展。根据国际研究预测，全球智慧农业的市场规模将从 2016 年的 90.2 亿美元达到 2025 年接近 700 亿美元的规模。

对于农业主要分支之一的渔业来说，投饵是非常关键的技术环节。随着养殖业的迅速发展，投饵机目前已被普遍应用，但存在着操作麻烦，灵活度低和投饵量难以准确控制等缺点，显然，对投饵机进行有效的改进是有必要的。

此外，在水产养殖过程中，不可避免的在很多水面上会漂浮许多垃圾，如园林垃圾、生活垃圾、工业垃圾等，在水面上一般很难实时地对漂浮垃圾进行收集处理。就目前而言，是通过拦漂拦截漂浮垃圾，然后通过手动清理。手动清理是清理水产养殖区漂浮垃圾的主要方式，手动清理一般是清理工人每天驾驶船只，利用网兜来打捞漂浮垃圾。传统的拦漂只能拦截漂浮垃圾并不能自动收集漂浮垃圾，需要手动清理拦漂拦截的垃圾。在进行手动清理漂浮垃圾的情况下，清理工人驾驶船只清理漂浮垃圾的效率低、打捞时间长、打捞次数少，并不能实时的保持河面的整洁。

（二）创新点与特色

Ⅰ.机械结构集成化

活动式料仓-自调节水下升降设计存放饵料的同时实现上浮下潜，一体式混料、输料及排料结构设计使多种功能共用一处电机实现，采用水泵式推进结构设计，替代现有四旋翼式推进。

Ⅱ.水产养殖智能化

以最小的人力付出，获得最大的经济效益。使用智能化的投喂器械无需人员看护，节省人力资源；无需观察鱼类生长状况、饵料食用情况即可使养殖对象获得科学、精准投喂量。

Ⅲ.渔业生产环保化

减少浪费的同时，清理水体污染。渔业养殖过程中盲目地，或者粗略地投放饵料往往造成水体内饵料过剩，且有机物堆积污染养殖环境。该产品科学的投饵技术可保证养殖对象健康生长的同时减少饵料浪费。此外，产品运行过程中可清理水面漂浮垃圾。

（三）过程中的体会与收获

无论是海洋牧场的建设还是淡水养殖、科研养殖基地，在养殖的整体环节中投喂饵料都是极为重要但费时、费力、消耗人工的工作；并且不科学的投喂频次、投喂饵料量均不利于渔业生产效益的提高。而人力打捞漂浮垃圾的传统方式更为劳累痛苦，且具有一定危险性。新型智慧渔业将助力各场景下的渔业养殖发展。

产品在运行过程中将对养殖水域实现实时、立体的监测系统，科研工作者可在养殖的同时以此为平台，利用全养殖过程中长期的、动态的水体环境监测数据结合鱼类生长状况等更好地发现、完善各类问题，助力科研领域的发展。

（四）项目实施的进程情况

1. 模型仿真测试

对机器结构进行适当的简化，并在 SolidWorks 中建模，然后将该模型导入 ANSYS Workbench 中。首先根据养殖过程中实际运行情况进行场景模拟，设定产品以 0.1 米/s 的速度下降，得到产品各部位承受的压力云图，如图 3.2 所示。然后根据模拟结果对产品模型施加载荷约束与边界条件，对其进行静应力分析，得到其应力与变形云图，如图 3.3、3.4 所示。

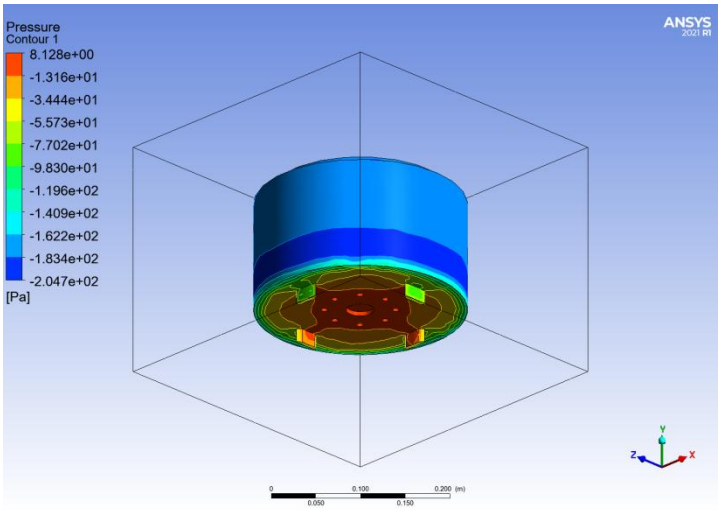

图 1.1 产品模拟运行受力云图

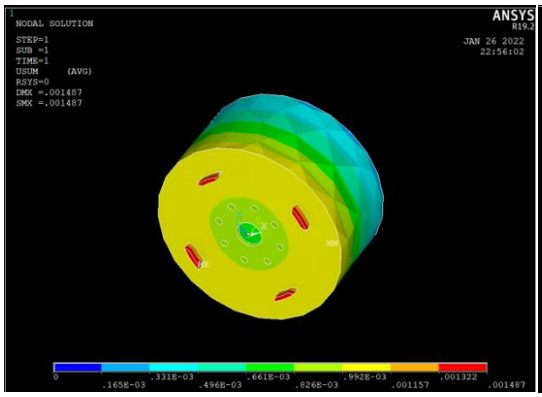

图 1.2 物体位移分析图

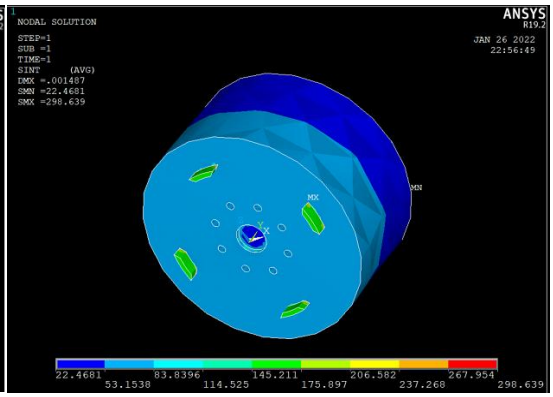

图 1.3 物体受力分析图

2. 实物制作与优化

a. 防水性

考虑到物体工作环境为水域，产品外壳采用一体式合金结构，保证良好的防水性能。此外，内部材料综合考虑成本等问题采用塑料为原材料，制作完成后对各部件进行封闭处理。

b. 负载性

考虑到产品的工作性质，产品材质需要一定强度来保障载重，同时尽可能减轻自身重量，优选地，外壳采用铝合金或不锈钢，实际制作过程中考虑到焊接所产生的精度问题、制作难度问题选用不锈钢为外壳材质，内部塑料材质的各结构采用 ABS 材料。

图 2.1 实物制作样品

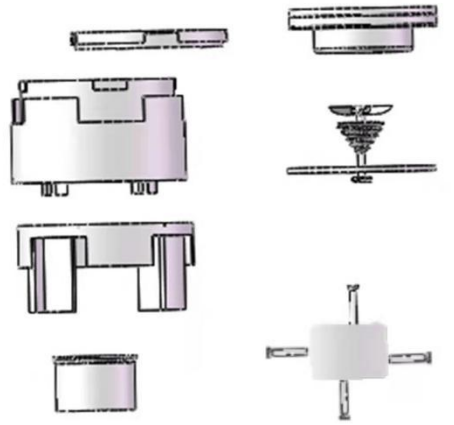

图 2.2 零件建模图

3. 实物初步运行状态测试

图 3.1 出水量测试

图 3.2 直行测试

图 3.3 转向测试

4.控制主体设计

产品控制部分由硬件控制层和软件模拟控制层两部分组成，主体控制简图如图 3.11 所示。

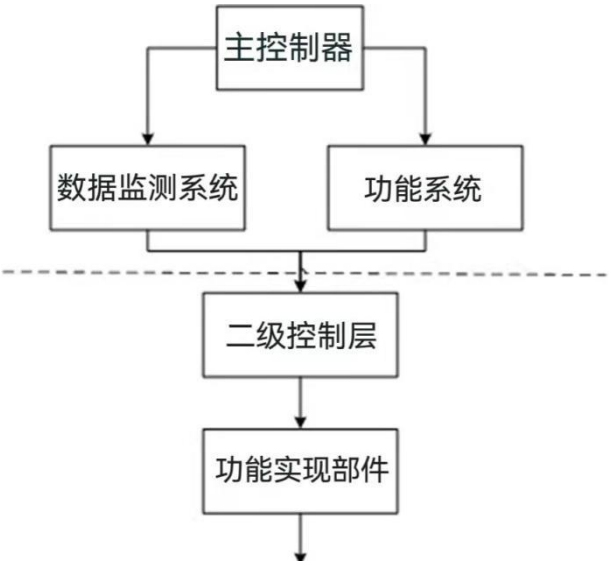

图 4.1 主体控制简图

硬件部分分为 stm32 主板、数据监测模块、恒源驱动模块、功能实现机械结构组成，实现流程如图 3.12 所示。通过产品搭载的温度、溶解氧等传感器与主控制器间的数据传递，实现数据实时监测，由主控制器对数据进行分析处理后发出机器运行信号，控制饵料投放的开始、暂停，控制浮筒升降实现对漂浮垃圾的收集或停止，控制机器巡航状态。

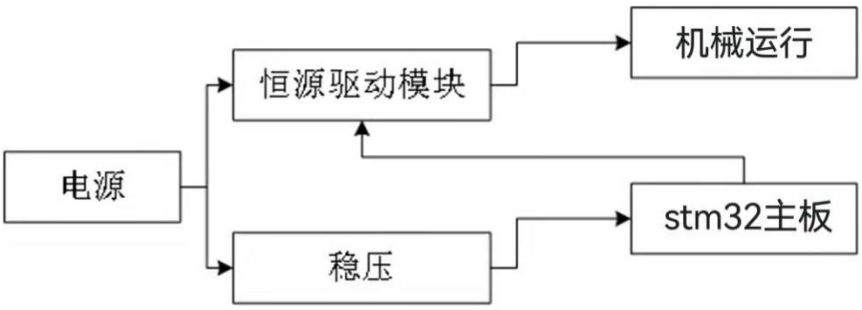

图 4.2 控制实现流程简图

```
    pidy.err = 0.0;
    pidy.err_last = 0.0;
    pidy.output = 0.0;
    pidy.SetAxis = 160;
    pidy.ActualAxis = 0.0;
    pidy.umax =100.0;
    pidy.umin = -100.0;
    pidy.integral = 0.0;
}

int x_axisPID_calculate()
{
    if(x_axis>30&&x_axis<270)
    {
        pidx.err =   pidx.SetAxis -x_axis ;
        pidx.output=pidx.Kp*pidx.err+pidx.Ki*pidx.integral+pidx.Kd*(pidx.err-pidx.err_last);
        pidx.err_last = pidx.err;
    }
    else
        pidx.output = 0;
//  if(pidx.output>60)
//      pidx.output = 60;
//  if(pidx.output<-60)
//      pidx.output = -60;
//  printf("    y_axis: %f   %d\n",pidx.output,pidx.err);
    return (int)pidx.output;
}

int y_axisPID_calculate()
{
    pidy.err = pidy.SetAxis - y_axis;

    pidy.output=pidy.Kp*pidy.err+pidy.Ki*pidy.integral+pidy.Kd*(pidy.err-pidy.err_last);
    pidy.err_last = pidy.err;

if(pidy.output>400)
    pidy.output = 400;
if(pidy.output<-400)
    pidy.output = -400;
printf("    y_axis: %f   %d\n",pidy.output,pidy.err);
return (int)pidy.output;
}
```

图 4.3 控制电机的 PID 算法程序

```
//定时器，用于实时控制
void Task_200hz_Thread(void)
{
    Remote_Control();                    //标定检测
    Check_All_Calibartion();             //状态指示灯运行
    Bling_Working(Bling_Mode);           //地面站
    StateMachine();                      //测量电池电压
    Get_Battery_Voltage();               //传感器状态机更新，检测航行器实时数据
    Statemachine_Sensor();               //PH测定仪
    Statemachine_PH_Meter();             //CTD温盐深仪
    Statemachine_CTD();                  //控制投饲
    Cabin();
}
```

图 4.4 实时模块化程序

（五）取得的成果

团队进行机械结构设计及 SolidWorks 建模，在 ansys 软件上进行模拟仿真，并搭建实物模型并下水测试。团队成员协作共进，积极参与科创赛事，取得了一定的比赛奖项。该项目完成了发明专利的授权以及外观专利的授权。

证书号第5406207号

发明专利证书

发明名称：一种水产养殖用浮漂垃圾收集与自动投喂智能机器人

发明人：崔秀芳;苑晓聪;魏仁杰;姜子昂

专利号：ZL 2021 1 1577948.X

专利申请日：2021年12月22日

专利权人：上海海洋大学

地址：201306 上海市浦东新区沪城环路999号

授权公告日：2022年08月26日　　授权公告号：CN 114190321 B

国家知识产权局依照中华人民共和国专利法进行审查，决定授予专利权，颁发发明专利证书并在专利登记簿上予以登记。专利权自授权公告之日起生效。专利权期限为二十年，自申请日起算。

专利证书记载专利权登记时的法律状况。专利权的转移、质押、无效、终止、恢复和专利权人的姓名或名称、国籍、地址变更等事项记载在专利登记簿上。

局长 申长雨

第1页(共2页)

其他事项参见续页

证书号第7761353号

外观设计专利证书

外观设计名称：垃圾收集航行器（水产养殖）

设计人：苑晓聪;魏仁杰;崔秀芳;陈成明;徐信;姜子昂

专利号：ZL 2022 3 0611811.0

专利申请日：2022年09月16日

专利权人：上海海洋大学

地址：201306 上海市浦东新区沪城环路999号

授权公告日：2022年12月20日　　授权公告号：CN 307739312 S

国家知识产权局依照中华人民共和国专利法经过初步审查，决定授予专利权，颁发外观设计专利证书并在专利登记簿上予以登记。专利权自授权公告之日起生效。专利权期限为十五年，自申请日起算。

专利证书记载专利权登记时的法律状况。专利权的转移、质押、无效、终止、恢复和专利权人的姓名或名称、国籍、地址变更等事项记载在专利登记簿上。

局长 申长雨

第1页（共2页）

其他事项参见续页

第十三届“挑战杯”上海市大学生创业计划竞赛结果

（同等级奖项以项目名称为序）

学校类别	学校	项目名称	拟授奖项	备注
普通高校	上海海洋大学	慧渔宝——科技服务三农，智慧振兴乡村	金奖	推荐国赛
普通高校	上海海洋大学	汇海洋——STEAM+理念下海洋教育践行者	铜奖	

图 1 第十三届“挑战杯”上海市大学生创业计划竞赛 金奖

图 2 第十一届全国海洋航行器设计与制作大赛长三角区域赛 三等奖

图 4 “六百光年杯”第十五届全国大学生节能减排社会实践与科技竞赛 全国三等奖

图 5 第七届上海市高校学生工业工程应用与创新大赛 一等奖

图 6 第十七届全国环境友好科技竞赛创业类 华东赛区一等奖

图 7 第十一届全国海洋航行器设计与制作大赛 全国一等奖

图 8 2022 年第十六届 iCAN 大学生创新创业大赛 上海赛区二等奖

数字工业设计大赛	上海海洋大学	沪城环路999	一种水产养殖用浮漂收集与智能投饵器	张丽珍、李俊	苑晓聪、魏仁杰、崔露雨、刘春雨、王根倩	二等奖
数字工业设计大赛	上海海洋大学	admition	独角兽高达	张莉君	哈国杨、孙扶霖、吴东豪、李博研、	三等奖
数字工业设计大赛	上海海洋大学	Butter Robot	黄油机器人	张莉君、沈伟	严梦昱、吕一	三等奖
数字工业设计大赛	华东理工大学	UCT创客	基于MPV的模块化座舱设计	刘晶	赵逸彬、雷聪锐、王少波、张洪巍、	三等奖
全国3D大赛3D/VR校园大使创新创业大赛	上海电机学院	/	/	邵兵、原恩桃	苏皖翼、曹芸豪、叶旭菁、李弈谋	三等奖

图 9 全国三维数字化创新设计大赛 上海赛区二等奖

图 10 上海市大学生“创造杯”大赛三等奖

实物演示

“中国魔方”——基于 TRIZ 理论的沙障铺设小车

案例分析

本大学生创新创业训练计划项目主要由三名机械设计制造及其自动化专业背景的学生为主导，在导师的悉心指导下，历经一年的时间从产品建模到项目路演，最后形成相关成果转化，锻炼了大学生的创新创业精神。在项目方面，为有效解决全球土地荒漠化的生态难题，针对现有治沙技术的不足，本大学生创新创业训练计划项目采用三维建模软件设计了一种以人为本、轻量化、便携式的直线型沙障铺设机器，以实现该装置从草料的储存，到开沟，再到送料，最后压草的流水线式工作模式。同时，又使用工业软件对关键零部件进行有限元分析，并验证其可行性，试验结果最终满足铺设要求。该产品的设计积极响应了“绿水青山就是金山银山”生态环保理念，有助于满足人民日益增长的美好生活需要，对促进区域经济协调、可持续发展、生态文明建设具有十分重要的现实意义。在收获体会方面，项目成员分析问题和解决问题的能力得到了提升，理解科创的意义在于过程而非结果，在创新中实现自我价值。

（一）项目的选题、目的与意义

通过铺设草方格建立防沙障是公认的最有效的工程治沙手段，但是目前我国草方格沙障布设的机械化程度较低，人工治沙存在劳动强调大、工作效率低、进度慢成本高等问题。本项目所提供的草方格沙障铺设技术，可以有效增加地表摩擦力，降低或缓解地表风速，从而抑制沙丘流动，起到固定沙丘的作用。在发挥其在防风固沙和保持沙土水分的最大效用的同时，为从事生态治理的企业及中间服务商提供技术参考，为沙区群众带去福祉，共建沙漠绿洲，努力践行“绿水青山就是金山银山”的生态环保理念，打造“中国魔方”。

基于相关专业和学科背景，学生自主导向，致力于推动乡村振兴取得新进展、农业农村现代化迈出新步伐。本项目不仅能够在国内进行沙漠的治理，帮助中国群众脱离沙漠化的威胁变现脱贫致富，还能在一带一路沿线进行其他国家国内的沙漠治理，帮助其他国家实现共同富裕的目标，推动中国一带一路经济计划的发展，对国际区域经济发展具有重大的意义。

（二）创新点与特色

（一）创新点

本项目的主要创新点在于通过行走装置、开沟装置、输草装置和压草装置之间的模块化配合。行走装置通过减速电机带动驱动轮，从而使整机实现全方位运动，整机两侧各安装有四套履带轮结构，采用履带轮使得整机拥有更好的通过性能；开沟装置的刀犁一端与四杆机构中的中间连杆固连，通过直流减速电机驱动双摇杆机构运动，可以使刀犁实现不同工作深度，并刀犁始终保持水平，以满足工作需求；输草装置分度滚筒和传送带工作，实现稻草分度、输送、定位；压草装置的升降部分根据齿轮传动具有传动平稳和传动效率高等优点，将直流电机作为动力源与升降架、齿轮、齿条结合组成升降装置，在竖直方向加入平行导向模组从而保证了升降过程的稳定性，通过升降功能可以满足工作过程中对压草深度的要求。总体结构上采用轻量化、高适应度、高机动性的设计理念，实用性好，实现精准治沙。

（二）特色

第一，项目产品本身采用了模块化设计，设计成可拆卸式，便于整机的安装与维护。第二，在电机支撑座等非标零件的制作上，我们采用了 3D 打印成型的技术方式，选用成本尽可能低廉同时又能保持生态环保的打印材料。第三，我们积极运用《机械原理》和《机械设计》课程所学到的专业知识，在开沟装置上，我们运用了双摇杆机构的机械原理，方案上选用了先开沟后压草的方式，能为后续压草环节省力；在压草装置上，我们运用了齿轮齿条配合的机械设计知识，通过调整齿轮齿条的啮合位置来控制压草深度以适应不同种地形。

（三）收获与体会

（一）项目申请

作为本科机械专业的学生，《机械原理》和《机械设计》是机械专业的核心课程，又正值大三的课程以专业素质综合能力培养为主，我们当时的想法就是“纸上得来终觉浅，绝知此事要躬行”，不能光以课内书本上的知识和优异的考试成绩为学习终点，更要将学习到的理论知识运用到实际中去，让书本上的知识得到升华，机械专业的学生更要培养自己的动手实践能力。机械创新设计大赛是机械专业的高水平赛事之一，正好以此次参赛题目为契机，从这一点，我们的收获是：在大学期间可能有不乏迫切想把学到的知识结合到实际的同学，但又不知道从何入手，那么这时，及时关注并搜集与本专业相关的科创赛事会是突破点之一。在众多科创比赛上，我们不仅能获得与高水平大学中的学生同台竞技的机会，与他们“切磋”并交流相关专业技能，还能获得企业专业以及知名教授的建议与点评，因此多多参加专业相关的科创比赛是一个提升大学生创新创业能力的很好机会。

在项目申请过程中，第二个让我们收获颇丰的点是在于团队的组建。我们的项目团队起初主要由三人构成，都是拥有较强的学习能力和创新创业精神，并且能够熟练运用本专业相关的软件，比如 AUTO CAD、SOLIDWORKS、KEIL 等等，还具有一定的单片机编程能力基础以及有其他赛事经验的同学。因此，在这一点上，我们的收获是：在开展创新创业计划过程中，团队成员的组建及架构是非常重要的。首先是需要一个领导者，即团队领袖，一般是项目的负责人和发起人，其需要有极强的领导能力、沟通能力和大局观意识，一般综合能力较强，比较善于分配任务和把控项目进度，另外，也需要有一定的信息收集能力，比如关注各大平台的赛事信息发布等等。其次是团队中的技术部门，一般工科类比赛会主要涉及到机械和控制两大内容，需要有较强的专业技能和知识，比如机械专业的同学需要拥有三维建模能力、空间想象能力和动手能力等等，负责控制部分的同学需要拥有单片机编程基础，熟悉各大开发板，同时，这两类同学在项目进展过程中还需要有很强的自学能力，因为开展项目遇到难题时，就需要借助网络视频教学、书籍等资源，自主解决遇到的难题。第三，团队中也需要有能说会道、口才伶俐的同学，项目答辩以及路演是他们展现自我的平台，当然，还要是赛事的类别情况，比如参加一些创业类赛事时，团队也需要招募一些经管类文科专业的同学来进一步提升团队实力。

（四）项目成果

经过团队成员与指导老师积极联系与沟通下，确定了实用新型和国际会议论文的两大撰写方向。于是，团队成员顺利开始着手专利申请书的撰写，期间涉及到专利权利要求书中专利图的部分，都是由团队成员运用 SOLIDWORKS 软件工程图的功能亲手绘制，并将初稿交由相关专业代理机构，形成最终稿专利权利要求书。

在国际会议论文方面，结合本创新创业训练计划项目的内容，在艾思科蓝论文平台检索关联度较高的国际会议，最终将投稿会议确定为第七届计算机技术与机械电气工程国际学术论坛(ISCME 2022)。论文投稿的过程是坎坷而又惊喜的，先将其中一次审稿意见记录如下：“文章未突出计算机与机械相关技术应用研究，理工科相关工程技术数据图表研究分析太少，建议文章（包括题目、摘要和关键词）可以往机械数据信息处理模型或计算机软件分析方向修改，重点突出计算机或机械实验技术应用，需要有具体的算法公式模型或相关实验研究数据分析。”于是，我们根据修改意见，将论文的主题及内容着重突出计算机与机械相关技术的应用研究，并加入相关公式和图表，积极阅读参考文献，学习国内外优秀论文的撰写风格与模式，期间我们的英语阅读和写作能力得到了提升，并且将科研工作中的严谨性牢记于心，这样的一个过程对我们今后无论是学习还是工作都是受益匪浅。

将投稿期间反复修稿、返稿的过程记录如下图所示，历经五次返修论文，最终于 2022 年 11 月 24 日收到论文录用通知，并顺利完成稿费缴纳。

第七届计算机技术与机械电气工程国际学术论坛 (ISCME 2022)

2022/11/25 - 2022/11/27 中国·杭州市

论 文 录 用 通 知

尊敬的作者：

您（们）好！ 很高兴地通知您，经过同行专家评审（评审意见详见系统附件），您投递的文章已被第七届计算机技术与机械电气工程国际学术论坛(ISCME 2022)录用。会议将于2022/11/25 - 2022/11/27在中国·杭州市举行，我们诚挚地邀请您出席会议并作口头报告或海报展示。

论文编号： VVRYF2ETFW
作者姓名： 杨尚青，施冬凡，汪子杰，胡庆松
论文名称： 以计算机软件为基础的新型沙障铺设小车研究

论文录用通知图

上海市机械工程创新大赛获奖证书图

iCAN 大学生创新创业大赛上海赛区获奖证书图

实用新型专利证书图

电动无尘黑板擦

案例摘要

项目成员有：潘金铎，胡治伟，洪弘，吴俊逸。所学专业有电气工程及其自动化，会计学，工业工程专业，为跨专业组队，有广泛的专业知识。项目指导老师：杨琛，副教授，研究方向为物联网大数据和智能控制技术、物联网技术、渔光互补技术。

由于近年来教师职业病率呈逐年上升的趋势，教师职业病呈现多样化方向发展，其中由粉笔粉尘引起的肺结核所带来的危害几乎可以和吸烟带来的害处相提并论。为了尝试解决该问题，保护师生健康安全，减少对环境的污染，项目对传统的黑板擦进行改造，项目改进传统黑板擦的内部结构，实现对粉尘的传输，清扫以及单向储存，较少粉尘的飘散。项目致力于改善黑板擦的使用手感，提供健康无尘的使用环境，解决擦拭过程中飞扬的粉尘，解决广大师生以及环保者的困扰。

通过项目的推进，我知道了项目计划以及团队的重要性，学会了更多的辅助技能，一个项目不止想法要好，在细节上也要不断打磨，更要弄清楚为什么这样设计，有没有更合理的设计方法，要注重每一个细小的结构，以及一个项目不是越复杂越高级越好，而是要用最简单的结构实现想要的功能。

一、项目的选题、目的与意义

该项目是在一次偶然的时间，接触到了飘落的粉笔末，于是想要通过对传统使用的黑板擦进行改进，以解决粉尘对于我们广大师生的困扰。项目通过底部安装滚轴式的软毛刷并利用人力实现对黑板的擦拭作用，在内部上层加装硬毛刷将附着于滚刷上的粉尘扫下，并通过内部静电吸附装置，进行吸引，辅助完成对粉尘的吸收，并在黑板擦上下两侧加装储存粉尘的特殊结构，在停止擦拭时使粉尘可以在内部自由运动，并在重力作用下进入粉尘储存的结构。在粉尘储存结构中设计具有独特功能的单向进入结构，使进入的粉尘无法溢出，并可通过装置的拆卸进行储存粉尘的倾倒。为解决飘出的粉尘，我们首先在黑板擦两侧加装软挡板，以避免粉尘飞散进而减少飞散。

二、创新点与特色

（一）改进传统黑板擦的内部结构，实现对粉尘的传输，清扫以及单向储存，较少粉尘的飘散

在设计过程中不断了解物理结构的设计技巧，并学习相应的建模，了解摩擦力的大小已经相应的轮转比的调节，协调轮转比和人力擦除之间的关系，做到用尽可能小的力，进行滚动擦拭并将擦拭的粉尘进行储存。

（二）改进黑板擦的外部形状，不拘泥于长方体外表，设计一个可阻挡粉尘附着人体的软挡板。

由于后面设计中考虑到黑板擦在使用过程中，经常手上附着粉尘，于是考虑在单独的黑板擦两侧加上距离黑板有一定距离的软挡板，使大多擦拭的粉尘贴着黑板，缩小粉尘的飞散范围，减少在手指上的附着。

（三）采用摩擦起电产生静电辅助粉尘的吸附，使板擦内部粉末的储存更高效。

由于考虑到仅仅依靠滚轴带动的惯性以及内侧清扫带来的阻力，可能不足以让粉尘高效的收集，但黑板擦内不便利用电能，就考虑用滚轴带动的方式产生摩擦起电，辅助粉尘的收集，在停止使用时会由于重力飘进粉尘的收集仓中。

最终有效解决广大师生的困扰并可有效的减少粉尘对环境的污染。

三、过程中的体会与收获

通过创新创业项目，熟悉了项目从想法到安排计划，再到一步一步检验自己的想法，最终达成项目预期的过程。以及团队的重要性，学会了更多的辅助技能，一个项目不止想法要好，在细节上也要不断打磨，更要弄清楚为什么这样设计，有没有更合理的设计方法，要注重每一个细小的结构，以及一个项目不是越复杂越高级越好，而是要用最简单的结构实现想要的功能。

在项目实践中，先不断的搜索去探寻项目的实现方法，因为想要去了解科创，培养创新思维，去了解别人想法的实现和技术的应用，看了往年的互联网＋的决赛，为之感到惊讶。在做项目的经历中，开拓了自己的思维。当时想出这个项目的时候才是大一，对技术懵懵懂懂，更不知道可以应用在哪些领域，在不断的学习和尝试中，培养了一些对此的认知，看到一个事物会想要剖析它的原理，了解它所应用的技术。

尝试过在项目中加入电动的器件，用现在的电能改变现在的技术，想要去用各种传感器和吸尘器实现黑板擦的功能，因此去学习单片机，以及各种传感器的应用，以及电机的安装。以现在想来，当时忽略了一个工具的实用价值以及成本。而一味的去让之变得复杂。经过了项目的流程熟悉，现在对于一个项目有了比较清晰的评判标准，知道一个项目应该怎么去做，以及怎么样才可以改良这个项目。

项目最初的想法比较的简单，经历了团队的一些团队交流，让这个想法变的完善。一个项目的完善不能缺少思维的碰撞，经过了不断的摸索，也取得了一些大大小小的进步，从最初的小方块，一步一步的改进，在内部加装设计机械结构，以实现想要实现的功能。经过不断的打磨推敲，项目初具雏形，也参加了一些比赛，比如互联网＋，汇创青春，上海市新特杯，上海海洋大学蔚蓝创新训练营。在比赛中不断寻找项目存在的问题，并不断地改进。项目也经历了很多的失败，在互联网＋中由于第一次写商业计划书，没有条理分明的写出自己想要表达的想法，但经历过，就对此有了一定的了解。在新特杯中，项目在市赛的答辩中，评委老师提出，我们缺乏原理性的解释，有的过于理想化，以及机械结构过于复杂，可能导致易损坏，以及说出了项目是用最简易的原理去实现自己想要的功能。在比赛之后也反思了自己的想法，去掉了一些不是那么必要的结构，减小结构的复杂度，降低成本，提高可行性。

经历了这次的项目，在未来再做项目的时候就明白了自己应该着重解决哪些问题，以及着重去看哪些问题。做项目一定要考虑应用，考虑成本。

四、项目实施的进程情况，取得的成果

项目的前期负责思路以及想法的交流和完善，在起初通过各种渠道了解这个项目是否有制作出来的一些成果，发现成果不多时，就开始尝试用自己的想法去设计改进黑板擦。

最初是用铅笔绘制草图，画出自己的大致构思以及想法，在不断地推敲中，设计了第一代的无尘黑板擦。也是用于申报大创时的设计构思，再后来团队学习三维建模软件，用于设计较为逼真的模型，并对之进行仿真，调节一些机械结构，协调好结构以及效率之间的天平。当时申报大创时还想把电的应用加入黑板擦，不过考虑到各种问题，比如成本，重量，以及充电过程的繁琐等，经过团队的交流，确定项目最终只利用机械结构方面的改良进行实现。我们开始搜索文献确定有必要的机械结构，加入了一些之间没加入的机械结构。然后又考虑到了手感方面的问题，在外形上进行改进，突破了常规的长方体黑板擦，用流鱼型的黑板擦作为外观，综合考虑了人手的握持以及与手部的贴合。开始着手撰写项目计划书以及商业计划书，但没有相关的知识储备，所以写的过程比较漫长。最好完成了第一版的商业计划书，做出了项目的第一个海报，并分别参加了互联网＋比赛和汇创青春比赛，只是遗憾都以失败告终。在一段时间的沉沦之后，开始去一些其他的比赛，在原本的基础上进行改进，加入减少手附着粉尘的软挡板，并考虑用静电进行辅助粉尘的吸附。参加了上海市第四届新特杯数字化创新设计大赛，以及第四届蔚蓝创新大学生科创训练营，有了一定的小的成果。

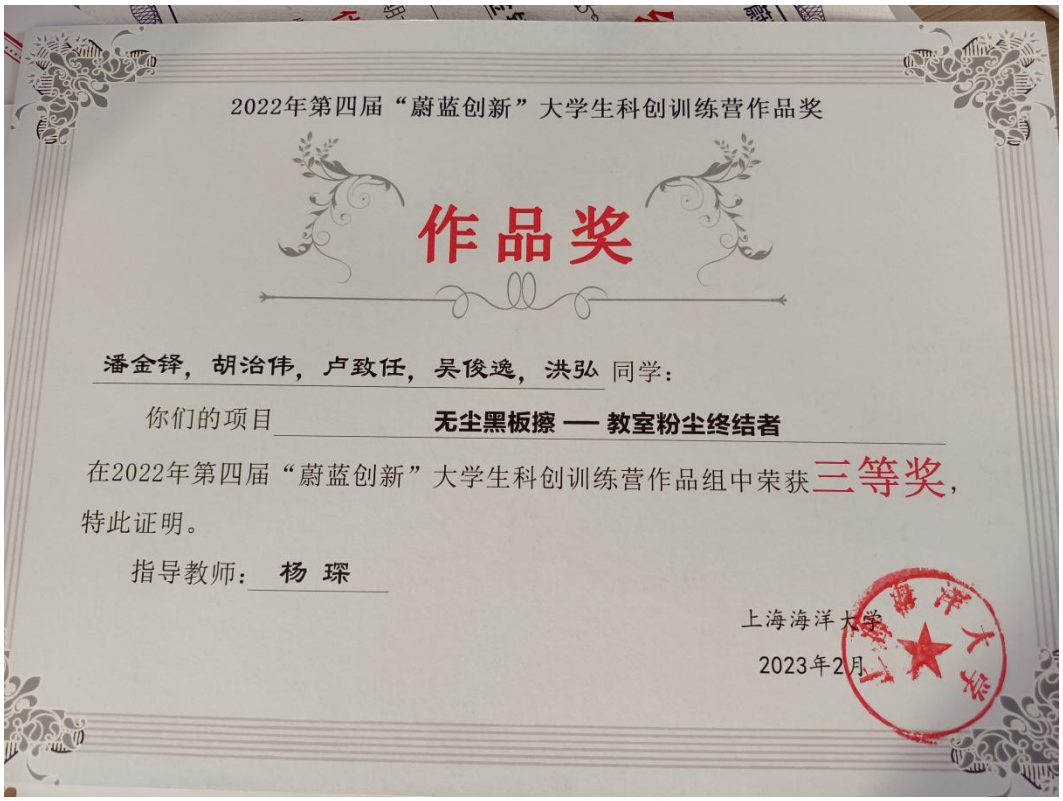

“蔚蓝创新”大学生科创训练营获奖证书图

上海市“新特杯”数字化创新设计大赛获奖证书图

基于雾化饵料投喂的立体监控养殖智能化水下航行器

案例摘要

本项目成员分别来自工业工程和行政管理，两位指导老师指导项目进行，各成员优势互补，掌握 51 单片机开发与 stm32 嵌入式开发技术，有 AutoCAD 二维建模经验和 SolidWorks 三维设计基础，掌握基础数模电、传感器技术、图像处理技术等专业知识，熟练掌握 C 语言编程和 MATLAB 仿真处理。项目指导老师陈成明教授和工业工程系上官春霞老师为专业学业导师，研究方向为渔业现代化，人机装备等方面，为项目的持续推进做出支持。陈成明教授主讲理论课《人因工程基础》和《基础工业工程》，实践课《人因工程独立实验》、《基础工业工程课程设计》、《工业工程创新原理应用设计》、《工业工程专业实习》、《专业综合能力提升实践》等实践环节。获上海海洋大学精品课程 1 门，上海市重点建设课程 1 门，认真负责对项目研究进行了指导。在项目的持续推进过程中，全体团队成员投入其中，锻炼了他们的团队协作能力，也让他们的理论知识得以学习致用，投入现实实践当中。

（一）项目选题目的和意义

本项目设计了一款基于雾化饵料投喂的立体监控养殖智能化水下航行器，以无人水下航行器作为研究对象，并根据系统需求设计了基于云平台的无人投饵远程监控水下航行器，完成了监控系统的整体结构设计、水样生物养殖系统的设计和各部分的软硬件设计。对该系统的研究有助于减小水产养殖业的劳动成本、提高水产养殖业的自动化和智能化水平，从而提高养殖户的经济收益，实现高效养殖、健康养殖和科学养殖。

水产养殖行业的商业价值数以亿计，并仍呈逐年上升趋势，本投饲系统将助力水产养殖发展，推动水产养殖向智能化、自动化发展，将该系统投入市场换来的利润十分可观。产品化后可以用于各渔业养殖厂、水产研究基地等。目前饲料制造产业工艺仍需要提高和改进，该装置应用于饲料用量和可用时长的监测，可以节省人力，提供饲料改进科学性数据，推动水产生物饵料制造工艺升级。产品化后可广泛应用于饵料开发工厂及相关科研机构。

（二）项目创新与特色

1、投饵方式智能化

对于投饲频率及投饲量的控制，以水质检测手段，将检测数据作为信号传达至控制对投饲进行控制。系统搭载 PH 测定仪监控水质，结合投喂量预测模型，按需定量精准投饲。

2、水下避障自主化

本产品搭载红外传感器并改进相应算法实现精准避障。此外，产品改进 PID 速度控制算法，进行水下航行器相关的速度调整，保持航行器稳定运行，辅助避障功能的稳定实现。

3、生态效益友好化

有机物的富集为水体污染的重要原因之一，而过量饲料往往难以处理，且养殖人员难以精准判断饲料的准确用量。本产品通过对投饲量的精准把控可以较好解决此类水体污染问题，并且在大规模使用后，实现对饲料及其原生产资源的有效节约。

（三）开展创新创业训练计划过程中的体会与收获

本产品的推进过程中考虑水生生物养殖环境，产品搭载水质检测装置。通过对养殖环境的水质中 TDS 值的变化判断水中所含离子状有机物的含量变化，从而作为水中饵料含量的依据，配合自动投饵模块的工作。同时，为减少天然环境的变化对饵料含量的判断造成误差，对水中的 ORP 值进行检测，主要判断消耗氧气的有机物(有害成分)，保障饵料含量判断的准确性的同时对养殖生物的生存环境实时监测，并通过数据传输在水质危害到生物生长时做出预警。此外，海水或淡水养殖以及对不同物种的养殖对环境的盐分以及 ph 值均有不同的要

求，通过对系统中不同物种的选择或手动输入调节，产品可对不同养殖对象有差别地监测并预警。但在研究过程并不知道如何将上述水质参数和自动化投饵相结合，因此经过多番查找文献，最终结合 BP 神经网络来进行投饵参数预测。

（四）创新创业训练计划项目实施的进程情况

（一）实施状况

1. 自动投饵技术

用于雾化饵料投喂。系统根据监控客户端发送的生物养殖信息和环境参数结合知识库中知识推理出饵料配方、投喂建议和投喂量。设计投喂量预测模型，通过 BP 神经网络模型结合水养生物的体态特征，水质环境和投喂率等条件预测饵料投喂量。当自动投饵模式开启时，下位机将传感器检测的数据通过通信系统传输至上位机，上位机根据基于 BP 神经网络的饵料投喂预测模型，以水温、酸碱度和溶氧量等参数为输入量，预测科学投喂量。上位机将此量反馈至下位机，下位机控制饵料投放机构进行投喂。从而实现了全自动的科学、精准投喂模式。

2. 实时监控系统

水样生物生长模型性能分析：训练过程中记录每次训练样本的误差和，绘制折线图观察误差的衰减速度。如图所示。横坐标代表训练次数，纵坐标代表训练样本误差和。

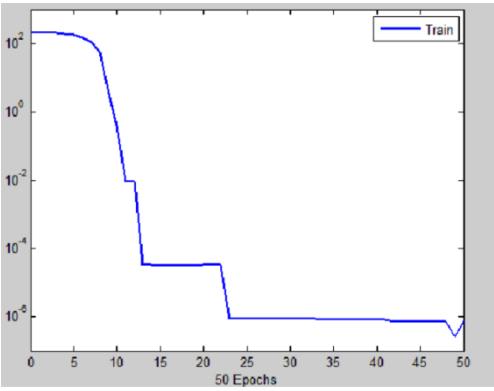

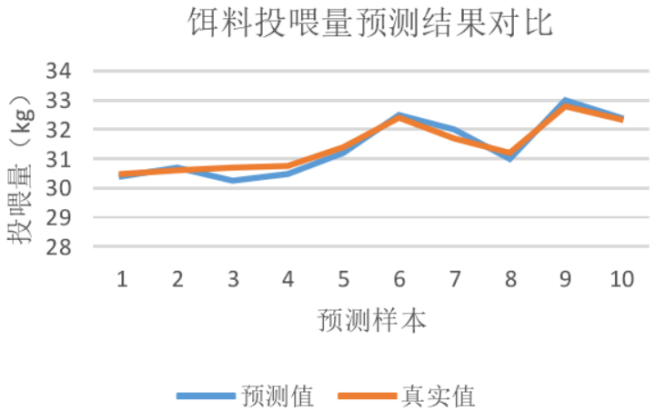

该网络经过 23 轮重复训练后达到期望误差。选取 10 组测试样本送入模型测试。测试完成后进行计算得到预测的饵料投喂量，将计算结果与真实结果进行对比。

3. 驱动及控制系统

在传统 PID 控制器的基础上，增加模糊规则，搭建模糊-PID 控制系统，以提高控制器在有干扰情况下的可靠性，从而增加航行器在复杂水域航行的可行性。在确定控制器的输入输出论域、确定各模糊变量的隶属度函数后，设计模糊逻辑规则，制定规则库，根据偏差量及其变化率、输入值获得输出，将采样参数带入模糊控制规则表进行解模糊，即可得到输出值。具体原理图如下所示。

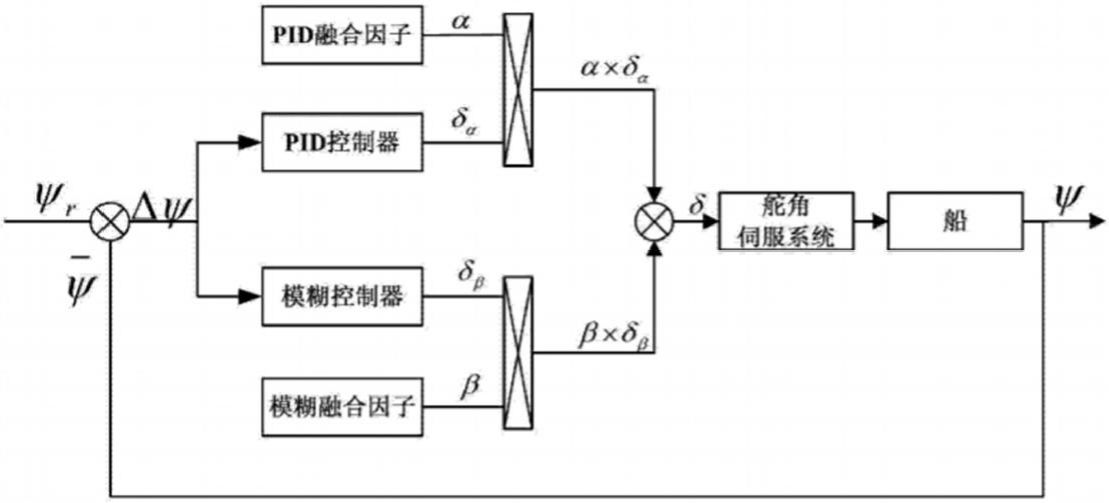

航行器通过搭载的红外线、陀螺仪等传感器获取实时环境信息并进行处理感知障碍船与本航行器的位置、运动方向以及运动速度，从而为避障算法提供精确的环境信息。激光雷达主要通过点云获取静态三维环境信息，为船舶动态避碰提供局部静态环境信息。通过坐标转换将各个传感器数据进行融合，进而丰富障碍物数据。随后根据算法计算出当前时刻下的船舶无碰撞的最优控制指令，实时在线对障碍船进行规避，当检测到有碰撞危险时，通过不断获取自身位置信息与障碍物信息，结合改进的动态窗口法计算出当前最优的航速与航向，从而控制本航行器对障碍船进行规避。

4.能源与动力系统

航行器的动力装置驱动器的额定工作电压为 12V，为了提高的航行器的续航能力，设计采用蓄电池进行供电，既方便又环保，电池规格要求是 12 伏特 105 安时。铅酸蓄电池构成主要包括正负极极板、隔板、电槽、电解液、池槽、蓄电池的上盖 W 及接线端子 W。其放电的化学反应是通过正负极板间的化学反应进行放电，将化学能转化为电能，电量不足时，可以加入相应的电解液进行补充。蓄电池是航行器的动力能源，为航行器的控制系统和信息采集系统提供电源。

电力推进系统经过进入的电能配电板来驱动航行器。它主要是有变频器、变压器、推进电机、螺旋桨、推进装置和推进装置构成。变压器能够让电站发出的电压转变为推进电动机所需的额定电压。转换器改变电压和电流的频率来控制推进电动机的转动速度。推进装置通过控制螺旋桨所产生的推力方向来作用于机体上。电能转变为机械能是靠推进电机，也要求功率要大，控制性能要好。

（二）项目完成状况及总结

在项目还没立项之前，团队成员大量查询了大量关于水下航行器，饵料的投放以及对水产生物的资料，因为大部分的知识是没有接触过的，前期的准备还是相对非常困难的，看什么都不会，但是随着对理论知识的学习和积累慢慢地就对该项目有了基本的框架和自己的见解，也是通过自己学习过的一些专业课知识和自己学习的一些其他领域的专业知识撰写了项目立项书，在成功立项之后，在实际操作的时候我们能清楚的发现，实际操作和理论的推理存在着较大的差距，我们需要更多的理论做为实践基础。一个人的能力有有限的，不同的人擅长的领域也是不同的，我们通过不同同学自己所擅长的能力才得以完成此项目，我们也是在此过程中收获了许多理论知识以及实践经验。也是通过本项目的研究使我们开始了解了学术研究以及对理论知识的梳理和联系。

（三）获奖情况

证书号第7975298号

外观设计专利证书

外观设计名称：输料桶（水产养殖）

设　计　人：魏仁杰;苑晓聪;陈成明;徐信;姜子昂

专　利　号：ZL 2022 3 0608028.9

专利申请日：2022年09月15日

专利权人：上海海洋大学

地　　址：201306 上海市浦东新区沪城环路999号

授权公告日：2023年04月07日　　授权公告号：CN 307957784 S

国家知识产权局依照中华人民共和国专利法经过初步审查，决定授予专利权，颁发外观设计专利证书并在专利登记簿上予以登记。专利权自授权公告之日起生效。专利权期限为十五年，自申请日起算。

专利证书记载专利权登记时的法律状况。专利权的转移、质押、无效、终止、恢复和专利权人的姓名或名称、国籍、地址变更等事项记载在专利登记簿上。

局长
申长雨

国家知识产权局

2023年04月07日

第 1 页 (共 2 页)

智能助老无人药盒

案例摘要

本项目四位成员分别来自电气工程及其自动化和物流工程专业，各成员从立项到资料收集、再到最后的成果整理，他们互相鼓励、互相扶持，有着面对困难时不放弃、乐观的精神。在导师刘雨青老师的帮助下他们设计并制作了一种长条鱼的自动化分拣打包装置，本装置通过传送带与包装机相结合的方式，创新地采用“自动分拣—加压加热—抽气密封“三个核心步骤进行长条鱼的打包，有效的解决了遇到的问题。随着改革开放的不断进行，我国的整体经济和科技都得到了迅猛的发展，人们的生活水平不断提高,从而对食品安全等都有了更高的要求。食品工业在近些年来发展迅速，这也是为了跟随时代的发展，满足人们的需求。在我国食品安全主要是由于食品包装不到位导致的问题，我国工厂鱼类打包大多采用人工，自动化程度低，安全保障也有所欠缺。对鱼类的自动化包装装置不仅可以保障食品安全，而且可以将鱼类包装生产与自动化生产相结合，降低劳动成本，提高企业效率。

（一）项目选题目的和意义

当前我国智能养老产品虽然种类丰富，但存在着严重的两极分化现象。低端产品市场进入门槛低，产品较多且大同小异;高端产品技术要求相对较高，但整个市场中，能量产高端智能产品的企业极少。随着智能养老设备有关技术的发展和大数据平台的完善，功能强大、花样翻新的智能健康养老产品将越来越多地出现在市场上,未来的智能养老设备产品也将越来越个性化。

由于老年人群中患有慢性老年疾病的人数众多,并且需要长期服用多种药物来控制和维持疾病的稳定，然而随着老年人人体机能的退化以及记忆力的减退，对于各种药物的服用剂量和服用时间等问题经常成为困扰老年人群里以及监护人的一个问题。因此，通过现在的高科技手段,设计一款可以通过简单设置就可以每天按时提醒并辅助老年人用药的智能药盒具有十分重要的研究价值和意义。

（二）项目创新与特色

1、空间可扩展性

每层包含三个药仓，用户可以单独购买增设层，以满足不同服药需求。

2、功能可扩展性

保留接口与不同医疗器械对接，打造基于物联网的家庭小型健康服务平台。

3、使用方式简便

用户只需要在听到铃声后，前往药箱位置，拿出自动弹出的药仓中的药物，根据语音提醒进行服用即可，简单方便，对老年人及特殊人群友好程度较高。

4、家用陪伴性强

市场上大部分医疗设施为专业医疗机构所有，并且以身体检查或护理为主，长期性家用设施较少。对于药品储存产品，市面常见为便携式，多用于外出携带，而本产品专注于家中固定使用。

此外，本产品为陪伴性，相比一般使用性器械对老人的操作能力要求较低，子女通过对产品进行预设，使老人几乎处于被动使用的状态。

5、综合使用性能高

一般药品储存设备功能较为单一,本产品在综合考虑老人普发疾病的情况增设血压及体温监测功能，此外出于子女对父母心理状况的关心增设对老人行动轨迹的关注。此外，一般医药箱采用塑料性合盖式，几乎不与外界隔绝，不利于特殊药物的存放。并且本产品为智能型装置， 相比传统医用箱更适合老人群体使用。

（三）实践过程

控制系统需要考虑电机控制、人机交互、通信和提示等模块，采用以 51 单片机为最小系统作为控制系统，可确保其实用和准确性。通过算法准确控制药物用量、是否服药、剩余服药次数等信息，以及服药定时定量的声光提醒，并通过通讯模块将用户的服药情况以及身体信息反馈给监护亲属。

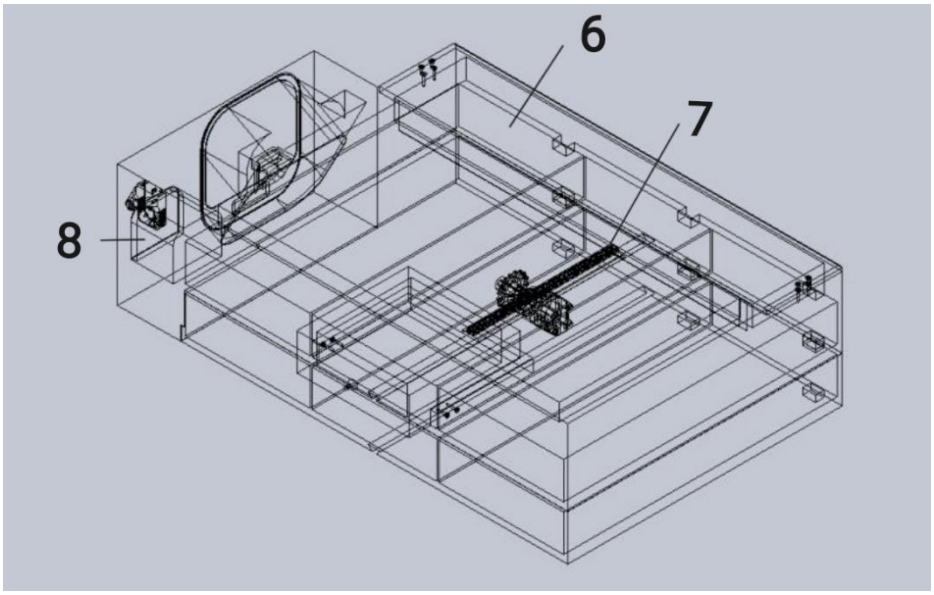

内部结构示意图

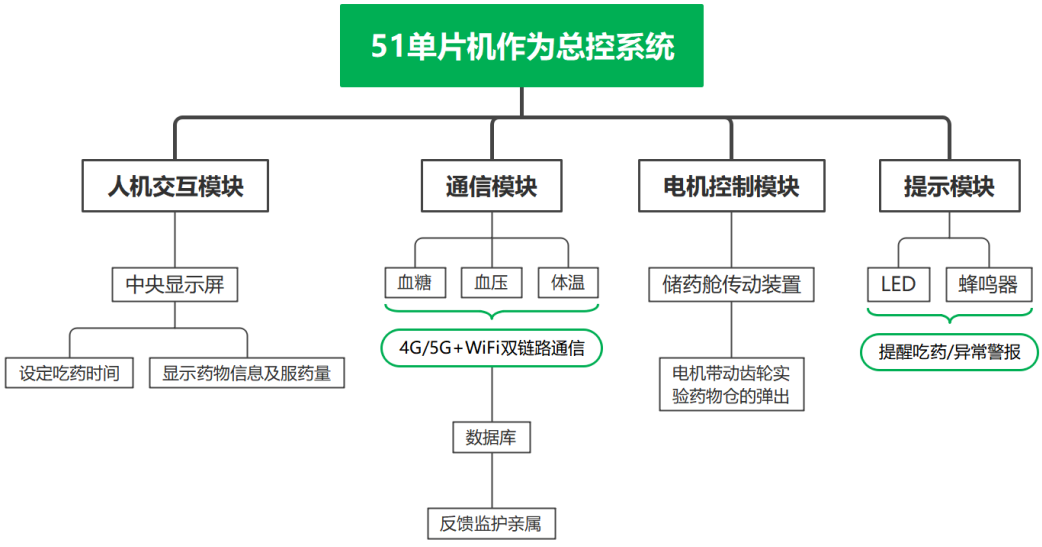

控制系统总体框架图

如图所示，以 51 单片机为总控系统，会在设定的吃药时间发出指令到储药舱传动装置，该装置在接收到指令后，由电机带动齿轮转动，实现对储药舱的弹出。电机驱动采用具有驱动能力强、发热量低，抗干扰能力强等特点的芯片。

人机交互模块由一块显示屏构成，吃药人可根据医嘱利设定吃药时间，显示屏会在到达吃药时间时显示药品种类和应服药品数量。

智能药箱通过 4G/5G+WiFi 双链路通信技术进行通信，与子女手机软件或者微信小程序

建立联系，能将采集到的老人的血压、血糖以及温度等数据予以可视化展示，并上传网络数据库当超过正常范围时会立即将信息反馈给子女，设计了 115200bps 波特率和 5Hz 电刷新频率保证信息处理速度，实现其时效性。

提示模块采用的是 LED 和蜂鸣器双重提醒方式，当达到设定时间时，单片机发出指令，LED 亮蜂鸣器响达到报警目的。

（四）项目成果

传统药盒关键较少用于行业应用，因为其不具备储存和数据传输的功能，所以其不具备可溯源的机制，智能药盒可广泛应用于健康管理机构、医院、科研机构等，一方面可以管理用户的真实服药状况，创新用户的服药习惯，使服药计划可以得到顺利实施；另一方面也可以根据用户的健康状况，实时调整用户的服药计划，减少过度治疗的状况发生；再者，用户的所有服药数据通过大数据分析整理后，可以完成机构药品用户机构的完整流通闭环，对行业发展具有重大的促进作用。而且随着经济发展，消费水平提高，医疗条件完善，使人口老龄化的增长，而老年人的记忆力减退，经常忘记吃药的时间。其实年轻人在面对着忙碌的工作的时候也常常会把吃药的时间忘记了，因此会耽误了病情。如果有了智能药盒以后，我们只需要调好时间，到点了智能药盒就会发出响声。这样就能提醒病人们吃药了。智能药盒是把智能手机 APP 与药盒结合在一起的产品，不仅可以盛放药品，还可以提醒人们按时吃药。随着人们生活水平的提升及消费需要的变化，智能药盒将逐渐成为每个家庭的共同需要，市场前景广阔。

表1国内典型药盒的功能设计分析

品牌	形状	价格（元）	分类功能	密封功能	便携功能	提醒功能	药量控制功能	监控功能
亿高 EKOA	扁圆	29.9	分格	双扣密封	便于携带	无	无	无
亿高 EKOA	胶囊	69	分格	双层密封	便于携带	无	无	无
欧润哲	圆形	19.9	分格	密封	便于携带	无	按天分格	无
加加林 JAJALIN	方形	19.9	分格	双层密封	便于携带	无	按天按顿分格	无
百家好世	方形	29.9	分层	单层密封	家庭使用	无	无	无
振兴	方形	59	分层抽屉	单层密封	家庭使用	无	无	无

市场现状及存在弊端：


图1 亿高 EKOA便携药盒


图2 欧润哲的旋转药盒


图3 Vilscijon维简提醒药盒


图4 沃穆定时语音电子药盒


图5 MEMO BOX智能药盒系统图

目前智能药盒的现状是刚刚起步，主要针对老年人，但随着对这种刚性的市场需求认识

的加深，市场一定会迎来一个发展热潮。

一开始出现的便携小药盒，造型简单，容量小，不能满足人们的需求，于是，随即又发展出现了大容量且功能齐全的药盒。随着逐渐更新完善，发展出现了造型多样的全新设计的人性化智能电子药盒，易操作，能定时，更简单。为更多人带来了便利。电子药盒不仅用于收纳不同的药片，这样也就拓展了电子药盒的消费对象，扩大了消费群体，提升电子药盒的使用价值。

以前大多电子药盒的电路通常由分立的数字电路器件组成，不仅功能单一，而且重量和体积都较大，特别是功耗大，提高了使用成本，因而具有很大的局限性。所以更加智能的电子药盒成为新的需要。

近几年，随着单片机技术的快速发展，以单片机为核心的大规模集成电路在各种产品中有广泛的应用。而以单片机为核心的数字电路正是由于具有功能丰富，体积小，功耗低等优势，符合电子药盒这一产品的特点，具有极大的市场潜力和开发价值。

而国内设计的智能药盒大多数属于提醒药盒又可称电子药盒、服药提醒器、计时药盒，是一种平时用于储放药物，并具备提醒人们按时服药的家用电子提醒及分药装置。（如图 3）Vilscijon 维简提醒药盒，采用定时闹铃式提醒患者服药，但在分类和药物药量的控制上没有解决老人服药的实际问题，分格少，药量容纳少。针对中老年人的家用式提醒药盒能够储放较多次的药量，一般按一月或一周的药量安排储药格（盒）。由于药量次数较多，故体积较大，不适合于外出携带，适合于须长期服食药物（或保健品）并有提醒需要的老年人、长期卧床者使用。（如图 4）沃穆的定时语音电子药盒，专为老年人设计，具有定时和语音提醒的功能，但是体积大，分格多，只适合家庭使用，不方便携带外出，另外没有随时监控的功能设计。这类药盒的优势：会提醒老人到服用药物的时间了。劣势：老人一般眼睛视力都不太好，无法分清药物的区别，容易误食药品。并且不能和医生互动，那么医生也不能开过多处方药，还是得频繁跑去医院。药盒的设计虽然很久前已经就出现了，但是智能药盒的研发还仍就处于开始阶段，设计者主要在外形、结构、色彩搭配上进行设计产品，而对于药盒的提醒、远程输入用药量用药时间、规范储存的研究涉及点还是比较少的。

一种用于滩涂养殖贝类采集与分拣一体智能化样机研发

案例分析

本项目生产研发的滩涂贝类养殖自动化一体装置，是一款适用于淤泥地，采集过程中可进行筛选的机械，有三大主要优势，其一是提高整个水域的滩涂贝类的产量。与现有采集方式相比。其二是减轻人工采集的劳动负担。本设计由采集装置、收集装置和控制部分组成，可以代替人工完成滩涂贝类的采育工作，提高效率。其三是用特殊转向的带挖槽的滚轮消除了原本通过人手持工具从上方破土对滩涂贝类造成的破坏。该设备方便操作，工作的深度可进行自动调控，可以通过一台机器实现采集、筛选多重功能于一身。

（一）项目选题目的和意义

目前滩涂贝类的采集方式主要为人工采集，人工效率低下且无法满足日益增长的滩涂贝类需求，大大限制了滩涂贝类产业的经济发展，因此本项目设计研发出一款滩涂贝类养殖自动化一体装置，能够有效解决这一痛点。

学生们通过日常生活观察与查阅资料发现，在其养殖到上市的过程中，采收环节主要依靠人工采集，而人工采集存在效率低下、成本较高、贝类容易遭到破坏的问题。基于对以上问题的思考，学生们产生了研发一种可以用于滩涂养殖贝类采收机器的想法，本项目应运而生。项目成员旨在通过研发这种机器达到高效、高质量完成滩涂贝类采收的目的，解决贝类养殖采收的相关问题。机器研发成功后具有降低采收过程中贝类损耗，减少人工成本，创造更好的经济价值的实用意义。

二、项目的创新点与特色

（一）技术创新

1.收集装置采用特殊耕犁形状

在众多滩涂贝类中，蛤蜊是其中养殖量最大且采收需求最迫切的物种，市面上贝类采集装置以蛤蜊采集居多。目前市面上的蛤蜊采集装置通常是三脚架形，适用场景单一，采集效率低。本装置通过耕犁旋动，可以轻松清除泥土，让蛤蜊暴露出来。同时可以适应各种地形，如沙地和淤泥地，在淤泥地质中的效率尤为突出。并且消除了原本通过人手持工具从上方破土对蛤蜊造成破坏的缺点。

2.高度自动机械化采集

整个装置采用了自动化设计，使用者只需按动几个按键即可实现全部功能。并且通过蓝牙模块实现作品与手机的物联，方便操作

3.通过一台机器实现贝类的采集、筛选、松土等多重功能于一身

与市面上功能单一的机器区别开，并且还实现了大中小贝类的分开处理，节省了大量人力。并且对于小贝类放生，也实现了环境友好的目标。

（二）市场创新

目前为止，人类对海底的探索只有 5%，还有 95%的海底是未知的。当前滩涂贝类养殖产业蓬勃发展，其中又以蛤类产业最具代表性，该产业的机器人制造业还是一片蓝海，市场需求量极大。

其次本项目可行性高。目前国内的贝类采集装置的零件尤其是高端精密零部件、芯片以及配套软件等依赖国外进口,受制于人。本项目采用的零件和模块均在市面可以找到，并且价格低廉，可以实现大规模生产。

本次项目利用水产养殖、机械制造、海洋蛤类养殖业等学科优势、实验室资源研发的用于滩涂贝类采集和收集智能化样机具有广阔的市场前景。

（三）项目实施的进程情况及取得的成果

在确定立项之后，我们就立即组织了一次会议，会议前我们搜寻整理了大量我们机器的前身--蛤蜊机的相关资料，在会议中，我们针对当前蛤蜊机可能存在的问题进行讨论，并提出了相应的解决方案，此次会议中，我们确定了对机器松土装置以及筛选装置进行优化，使其能够应用于更多诸如蛤蜊的滩涂贝类的采集。此次会议之后在执导老师张俊的牵动下，我们又与在机械制造颇有建树的张宁学长进行了一次讨论，主要是对本机器的优化改动的可行性进行分析，本次会议结束之后我们基本确定了机器设计思路，并绘制了三维模型图。

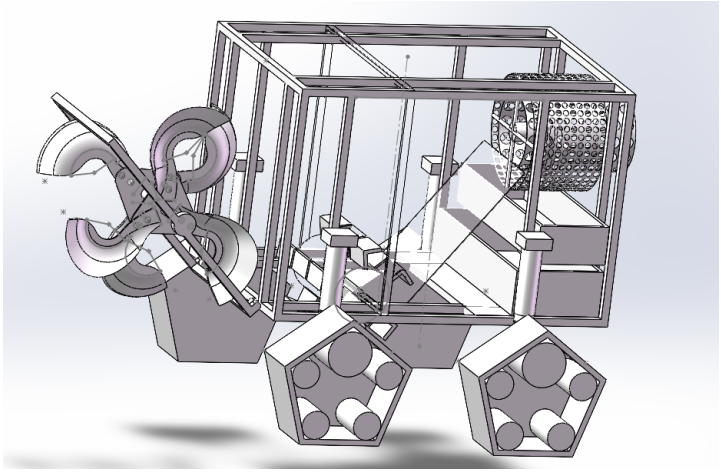

图 1 第一版三微模型图

制作完成第一版模型图，如图 1 所示，我们与老师进行一次讨论，老师指出作为驱动装置的履带设计上存在缺陷，这种履带设计虽然在凹凸不平的地面上有着不错的表现，但是在机器主要工作的泥沙地上会因为接触面积不足容易下陷。听取老师建议后我们立即修改完善，重新设计了驱动装置，并且在之后研究发现，冲水装置在机器中比较累赘，于是我们将其从我们的机器中舍去。最终，经过数个月不断的研究改进，我们完成了我们机器最终的三维模型绘制，如图 2 所示。

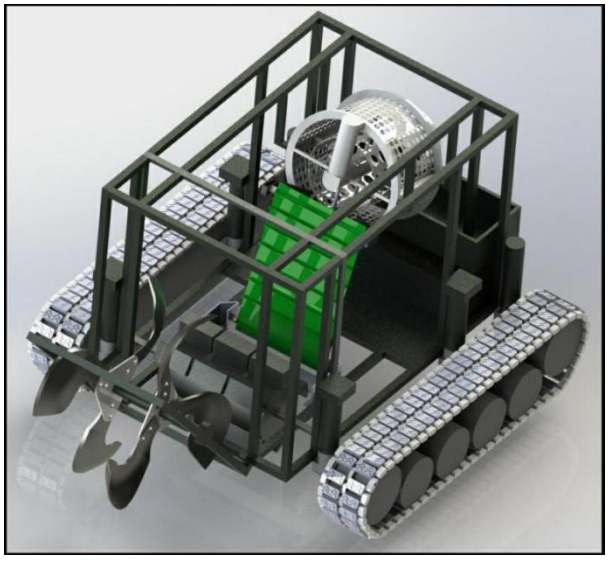

图 2 最终版三维模型图

机器由驱动装置、松土装置、采集装置、筛选装置、收集装置、控制装置组成。在进行采收工作时，先由松土装置将贝类上方的泥土扒开，再由采集装置采收，并通过传送带运送至筛选装置，将贝类按体型大小筛分，最后在收集装置进行短暂的储存。

如图 所示为松土装置，采用开沟轮设计，能够有效将贝类上方的泥沙拔开至两旁，使

贝类暴露在采集装置前，方便采集，同时减少采集贝类时附带的泥沙量。

图 3 松土装置图

如图 3 所示为采集装置，采集装置包括多个弯杆,用于将贝类从泥土表面挖掘出，在挖出贝类后，将贝类短暂存放至传送带下方的收集盒中，贝类经过收集盒到传送带上，由传送带传送到筛选装置。

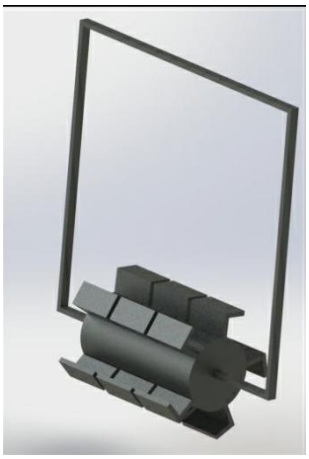

图 4 采集装置图

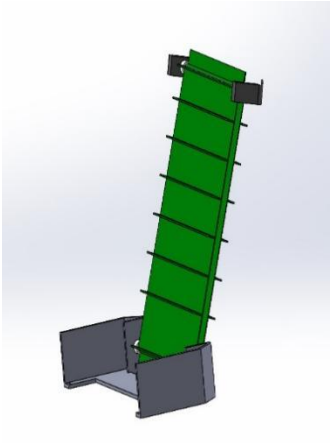

图 5 采集装置图

图 4 和图 5 筛选装置，筛选装置采用双重带孔洞滚筒设计，内一层滚筒上带有直径 40mm 孔洞，用于筛选体型较大的贝类，体型较大的贝类不会穿过孔洞，并且由于滚筒不断旋转，也不会卡在孔洞上，最后在重力的作用下，滑入收集装置。体型中等的贝类将穿过内一层滚筒来到外一层，同理内一层滚筒的筛选原理，将体型中等与体型小的贝类筛分，体型中等的贝类将滑入收集装置，体型小的贝类将直接放生会泥沙中，继续生长。收集装置由两层，上层收集体型较大的贝类，下层收集体型中等的贝类。

图 6 筛选装置图

在完成了三维模型图后，我们尝试着参加了一些比赛，比如互联网+，挑战杯，汇创青春，但比较可惜的是我们仅仅拿下了互联网+校赛的奖项。

失败并未打击到我们，接下来我们开始进行实物的制作。在实物的制作的过程中我们发现想要实现我们的设计，并非一件简单的事情，我们需要的材料很难买到现成，往往需要定制，但研究经费不允许我们将机器每一个部件定制出来，我们不得不重新做图纸设计，在不影响机器的大体架构上，做一些细节上的补充、调整，以降低制造的成本。在制作过程中我们遇到最大的困难莫过于疫情，我们大创期间正值疫情肆虐，也因此我们实物的制作一度陷入长时间停滞。尽管截至结项，我们实物的制做仍然未能完成，但我们会坚持下去，将机器完成。

（四）获奖成果

3. 大学生创新创业项目经费管理办法

上海海洋大学工程学院大学生创新创业计划项目经费管理办法

（试行）

第一章 总则

第一条 为规范大学生创新活动计划项目经费的管理，提高资金使用效率，根据《上海高校大学生创新活动计划实施办法》和学校有关财务规章制度，制定本办法。

第二条 大学生创新活动计划省市级项目经费来源于上海市财政拨款，校级项目经费来源于学校预算。

第三条 项目经费管理和使用原则

科学安排，合理配置。要严格按照项目的目标和任务，科学合理地编制和安排预算，杜绝随意性。

专款专用，专人负责。指导老师和各项目负责人（学生）是创新项目经费的主要责任人，各项目负责人（学生）网上填报经费报销单后，经指导教师同意，各项目负责人（学生）签字，指导老师签字后，报工程学院领导审核签字，确保专款专用。

第四条 项目完成后学院组织结题工作，结题报告中应包含项目经费预算执行情况。

第二章 项目经费开支范围

第五条 项目经费是指在项目组织实施过程中与创新活动相关的、由专项经费支付的各项费用。

第六条 项目经费的开支范围一般包括设备费、材料费、测试化验加工费、图书资料费、办公用品费、印刷费、差旅费、出版/文献/信息传播/知识产权事务费等。

设备费：是在指项目研究过程中购置或试制专用仪器设备，对现有仪器设备进行升级改造，以及租赁外单位仪器设备而发生的费用。由于学校的示范性实验中心、各类开放实验室与重点实验室均向参与项目的学生免费提供实验场地和实验仪器设备，项目经费需严格控制设备购置费的支出。

材料费：是指在项目研究过程中消耗的各种原材料、辅助材料等低值易耗品的采购及运输、装卸、整理等费用。

测试化验加工费：是指在项目研究过程中支付给外单位的检验、测试、化验及加工等费用。

图书资料费：是指在项目研究过程中购置与项目研究相关的书籍、文献资料，一般不超过项目总经费的 5%。

印刷费：是指在项目研究过程中用于打印、复印项目资料、调查问卷等所需的费用，理工农类课题此类支出一般不超过项目总经费的 8%，文经管类课题一般不超过项目总经费的 12%。

差旅费：是指在项目研究过程中开展科学实验（试验）、科学考察、业务调研、学术交流等所发生的外埠差旅费、市内交通费用等。其标准应当按照学校有关规定执行。

出版/文献/信息传播/知识产权事务费：是指在项目研究过程中，需要支付的出版费、资料费、专用软件购买费、文献检索费、专业通信费、专利申请及其他知识产权事务等费用。

第七条 项目研究过程中发生的除上述费用之外的其他支出应当在申请预算时单独列示，单独核定。

第三章 项目经费奖惩办法

第八条 项目经费采取阶梯式发放制度。项目成功立项后首先发放经费的 50%。如项目在中期检查结束前提前完成，可以向工程学院科创管理老师申请提前检查发放剩余经费。

第九条 学院会进行项目中期进度检查，根据考核结果发放后续经费。考核内容如下：

（一）项目经费使用情况：是否使用已发经费的 50%以上（包括 50%），学院系统导出数据；

（二）创新创业类竞赛参与情况：是否报名附件 1 所列比赛，需提交成功报名参赛的证明材料；

（三）论文发表情况：是否发表论文，需提交接收函作为证明材料；

（四）专利发表情况：是否发表专利（包括发明专利、实用新型专利），提交专利受理通知作为证明材料；

（五）项目开展情况：根据提交的材料（包括研究报告、实物模型、视频等）对项目开展情况进行评估；

（六）其他：项目开展期间，工程学院将开展至少四次大创相关活动（项目经费使用培训、科创思维课、中期检查例会、科创论坛等），组织签到。中期检查会安排指导老师座谈，项目负责人给指导老师汇报，指导老师给出原创性评价。

第十条 针对项目开展情况较好的组别，将在原有经费的基础上，额外增加项目经费，封顶至总经费 50%：

	国家级	省市级	中期检查
一等奖	20%	15%	10%
二等奖	15%	10%	8%
三等奖	10%	5%	5%

（一）项目在附件 1 所列比赛中获得由团中央、教育部、中国科协、全国学联、省级人民政府（含直辖市）主办的各类国家级竞赛的决赛一、二、三等奖，每个项目每个比赛分别增加总经费 20%、15%、10%；获得由省（含直辖市）委及以上、教育部各类教学指导委员会、各省教育厅（含直辖市教育委员会）主办的各类市级竞赛的决赛一、二、三等奖，每个项目每个比赛分别增加总经费 15%、10%、5%；项目在中期检查中获得一、二、三等奖，每个项目分别增加总经费 10%、8%、5%；

（二）项目获得实物，并且被院级及以上公开展出，每个项目增加总经费 15%；

（三）发表与项目成果相关的论文（要求见刊），且前三作者有项目组成员，每个项目增加总经费 15%；

（四）发表与项目成果相关的专利（要求公开），且前三作者有项目组成员，发明专利每个

项目增加总经费 15%，其他专利，每个项目增加总经费 5%。

（五）以上增加额度必须和项目有关，且需提前三天由项目负责人填写工程学院本科生创新创业项目经费提额申请表（附件 2）并附上证明材料发至科创管理负责老师审核，审核通过后发放。

第十一条 针对项目开展情况较差的组别，将在原有经费的基础上，扣除后续经费，扣完即止：

（一）项目经费使用情况：项目经费使用未达到已发放经费的 50%且没有成果（竞赛获奖、论文、专利、实物），则将后续经费全部扣除；

（二）比赛参与情况：项目未参与“互联网＋大学生创新创业大赛”，则将后续经费全部扣除；

（三）其他：开展大创相关活动，每次活动至少一名项目成员参加，缺席一次给与警告，缺席两次及以上给与处罚；

（四）项目接到投诉或者举报，项目成员应提供证明材料，如发现确实存在学术不端、违规违纪和不公平竞争，经费全部扣除，并追究相应责任，按照校规校纪给与处分。

第四章 监督检查

第十二条 工程学院对专项经费拨付使用情况进行监督检查，如果与学校规章有出入，以学校规章为准。

第十三条 对于预算执行过程中，不按规定管理和使用专项经费、不及时编报预算、不按规定进行报销的项目实施小组，工程学院处予以停拨经费或通报批评，情节严重的可以终止项目。

第五章 附则

第十四条 本办法由工程学院负责解释。

第十五条 本办法自发布之日起施行。

附件 1 创新创业竞赛

国家级竞赛名称	省市级竞赛名称
中国国际“互联网＋”大学生创新创业大赛	上海市“互联网＋”大学生创新创业大赛
“挑战杯”全国大学生课外学术科技作品竞赛	“挑战杯”上海市大学生课外学术科技作品竞赛
“挑战杯”中国大学生创业计划大赛	“挑战杯”上海市大学生创业计划大赛
全国大学生创新创业训练计划年会展示	上海市大学生创新创业训练计划成果展
“创青春”全国大学生创业计划大赛	“汇创青春”—上海大学生文化创意作品展
全国大学生智能汽车竞赛	陈嘉庚青少年发明奖(上海)
国际大学生 iCAN 创新创业大赛	上海高校学生创造发明“科技创业杯”奖
国际海洋工程装备科技创新大赛	“上汽教育杯”上海市高校学生科技创新作品展
全国三维数字化创新设计大赛	全国三维数字化创新设计大赛（上海赛区）
	上海市大学生“创造杯”大赛
	上海市大学生机械工程创新大赛
	上海市先进成图技术与创新设计大赛
	“创青春”上海市大学生创业计划大赛

二、竞赛获奖统计表

2022 国家级竞赛获奖

序号	学生姓名	作品名称	竞赛/论坛名称	获奖级别	奖项等次
1	姜嘉辉	大学生数学建模竞赛	美国大学生数学建模竞赛（MCM/ICM）	国家级	二等奖
2	黄宝辉	大学生电商物流与供应链创新	SCMWAY 全国大学生电商物流与供应链创新精英挑战赛	国家级	一等奖
3	田昱彤 梁培琪 刘雨佳	大学生电商物流与供应链创新	SCMWAY 全国大学生电商物流与供应链创新精英挑战赛	国家级	二等奖
4	栗云帆 吴欣雨 王邱杰	大学生电商物流与供应链创新	SCMWAY 全国大学生电商物流与供应链创新精英挑战赛	国家级	二等奖
5	魏仁杰	全国大学生创业	挑战杯全国大学生创业竞赛	国家级	三等奖
6	崔雪飞 黄万林 陈荣	大学生电商物流与供应链创新	SCMWAY 全国大学生电商物流与供应链创新精英挑战赛	国家级	一等奖
7	白浩然	大学生数学建模竞赛	全国大学生数学竞赛	国家级	一等奖
8	陈慕尧	大学生电商物流与供应链创新	SCMWAY 全国大学生电商物流与供应链创新精英挑战赛	国家级	二等奖
9	陈逸凡	大学生数学建模竞赛	全国大学生数学竞赛	国家级	一等奖
10	鲁彪	大学生电商物流与供应链创新	SCMWAY 全国大学生电商物流与供应链创新精英挑战赛	国家级	

11	宛晓聪	全国大学生创业	挑战杯全国大学生创业竞赛	国家级	三等奖
12	万易函 李兰奇	大学生电商物流与供应链创新	SCMWAY 全国大学生电商物流与供应链创新精英挑战赛	国家级	一等奖

2022 省市级竞赛获奖

序号	学生姓名	作品名称	竞赛/论坛名称	获奖级别	奖项等次
1	李文亮	医用循环箱运营网络系统设计	“云丰杯”全国绿色供应链逆向物流设计大赛	省市级	二等奖
2	杨扬	大学生工业工程应用与创新	上海市大学生工业工程应用与创新大赛	省市级	二等奖
3	潘金铎	单片机设计与开发	蓝桥杯全国软件和信息技术专业人才大赛（电子类）（上海赛区）	省市级	一等奖
4	赵宏钦	大学生工程实践与创新能力	在第十二届上海市大学生工程实践与创新能力大赛	省市级	一等奖
5	哈国杨	三维数字化创新设计	全国三维数字化创新设计大赛	省市级	三等奖
6	李博研	三维数字化创新设计	全国三维数字化创新设计大赛	省市级	三等奖
7	常艺远	大学生工程训练综合能力	上海市大学生工程训练综合能力竞赛	省市级	一等奖
8	冯骏	单片机设计与开发	蓝桥杯全国软件和信息技术专业人才大赛（电子类）（上海赛区）	省市级	二等奖
9	和远航	大学生工程训练综合能力	上海市大学生工程训练综合能力竞赛	省市级	二等奖
10	王浩然	大学生机械工程创新	上海市大学生机械工程创新大赛	省市级	二等奖
11	陈逸凡	大学生数学竞赛	全国大学生数学竞赛	省市级	一等奖

12	曾瑞琪	大学生数学建模	全国大学生数学建模竞赛	省市级	三等奖
13	胡治伟	单片机设计与开发	蓝桥杯全国软件和信息技术专业人才大赛（电子类）	市级 C	三等奖
14	孙扶霖	三维数字化创新设计	全国三维数字化创新设计大赛	省市级	三等奖
15	吴东豪	三维数字化创新设计	全国三维数字化创新设计大赛	省市级	三等奖
16	黄晶晶	遇见那片“Ocean”——海洋科创教育助力“双减”	“知行杯”上海市大学生社会实践大赛	省市级	三等奖
17	黎民赞	单片机设计与开发	蓝桥杯全国软件和信息技术专业人才大赛	省市级	三等奖
18	张成强	SHOU	全国三维数字化创新设计大赛	省市级	一等奖
19	朱楚亮	多功能水下机器人	全国三维数字化创新设计大赛（上海赛区）	省市级	一等奖
20	刘彦男	工程训练综合能力	全国大学生工程训练综合能力竞赛	市级	二等奖
21	周雅婷	工程训练综合能力	全国大学生工程训练综合能力竞赛	市级	二等奖
22	王宇恒	三维数字化创新设计	全国三维数字化创新设计大赛	省市级	一等奖
23	倪榕键	单片机设计与开发	蓝桥杯全国软件和信息技术专业人才大赛（电子类）（上海赛区）	省市级	三等奖
24	徐伟钤	基于手机 APP 实时计费的景区智能跟人小车创业计划研究实施	蓝桥杯全国软件和信息技术专业	省市级	一等奖
25	陈晟	大学生机械工程创新	上海市大学生机械工程创新大赛	省市级	一等奖
26	哈国杨	“长江口”中大型鱼类 3D 仿真及 AI 识别	全国三维数字化创新大赛	上海市	三等奖
27	曾瑞琪朱哲慧	一种智能安全帽的设计	第七届上海市大学生工业工程应用与创新大赛	上海市	三等奖
28	曾瑞琪朱	一种智能安全帽的设	第七届“汇创青春”	上海市	三等奖

	哲慧王涵涵	计			
29	曾瑞琪朱哲慧	一种智能安全帽的设计	第十六届 iCAN 大学生创新创业大赛	上海市	三等奖
30	陈长张文峰卢梁羽骐	基于物联网的智能花卉养护系统	ICAN	上海市	三等奖
31	张涛涛	水面水下两用小型救援航行器	第十一届上海市大学生机械工程创新大赛	上海市	二等奖
32	陈天野徐文静龚子涵	基于自动智能地锁的共享云平台系统	第十二届全国大学生电子商务“创新、创意及创业”挑战赛上海赛区省级选拔赛	省市级	一等奖
33	朱子豪胡彦	基于 IOT 物联网技术的环保污染治理配电终端研究	2022 年上海市大学生电子设计竞赛	省市级	三等奖
34	刘俊辰殷之抗付文森	便携消防水带收纳机	新特杯数字化创新大赛	省市级	三等奖
35	施冬凡汪子杰杨尚青	“中国魔方”——基于 TRIZ 理论的沙障铺设小车	第十一届上海市大学生机械工程创新大赛	上海市	一等奖
36	施冬凡汪子杰杨尚青	“中国魔方”——基于 TRIZ 理论的沙障铺设小车	2022 年第十六届 iCAN 大学生创新创业大赛上海赛区选拔赛	上海市	二等奖
37	魏仁杰张可欣苑晓聪	一种水产养殖用浮漂垃圾收集与自动投喂智能机器人	第十七届全国环境友好科技竞赛	省市级	一等奖
38	魏仁杰苑晓聪徐信	一种水产养殖用浮漂垃圾收集与自动投喂智能机器人	第七届上海市高校学生工业工程应用与创新大赛	上海市	一等奖
39	魏仁杰苑晓聪徐信	一种水产养殖用浮漂垃圾收集与自动投喂智能机器人	2022 年第十六届 iCAN 大学生创新创业大赛	上海市	二等奖
40	苑晓聪魏仁杰崔露雨	一种水产养殖用浮漂垃圾收集与自动投喂智能机器人	全国三维数字化创新设计大赛	上海市	二等奖

41	徐信魏仁杰苑晓聪	一种水产养殖用浮漂垃圾收集与自动投喂智能机器人	上海市大学生“创造杯”大赛	上海市	三等奖
42	李路阳陆嘉波王韶洋	面向用户行为能力分析的智慧衣架	ICAN 大学生创新设计大赛	上海市	
43	周琪 朱梦祥	一种废玻璃瓶回收装置的设计	全国三维数字化创新设计大赛	上海市	特等奖

2022 校级竞赛获奖

序号	学生姓名	作品名称	竞赛/论坛名称	获奖级别	奖项等次
1	梁丽敏	智能饲料盘研究及设计	渔业装备创新设计大赛	校级	三等奖
2	陈柄良	大学生科创训练	2022 年第四届“”蔚蓝创新”大学生科创训练营	校级	二等奖
3	黄宝辉	湖面清洁气垫船	三维数字化创新设计大赛	校级	三等奖
4	张涛涛	水面辅助救援航行器	上海海洋大学三维数字化创新设计大赛	校级	三等奖
5	俞锦松	《卿心相助——大学生朋辈互助共促平台》	2023 临港地区高校“创新生涯·驱动人生”大学生创新训练营定向越野路演	校级	二等奖
6	胡治伟	无尘黑板擦——教室粉尘终结者	2022 年第四届“蔚蓝创新”大学生科创训练营作品奖	校级	三等奖
7	罗后洪	贻贝采收清洗设备	渔业装备创新设计大赛	校级	二等奖
8	周雅婷	“神农铠甲”无人植保机	2022 年第四届“蔚蓝创新”大学生科创训练营作品奖	校级	二等奖

三、学术论文

1. 公开发表论文统计表

序号	作者姓名	发表论文名称	刊物名称	期次
1	崔雪飞	A VMD-MSMA-LSTM-ARIMA model for precipitation prediction	Hydrological Sciences Journal	2

2. 论文全文汇编

A novel combined VMD-MSMA-LSTM-ARIMA model for data-driven deep learning in precipitation prediction

Xuefei Cui[a], Zhaocai Wang[b]* and Renlin Pei[b]

[a]*College of Engineering, Shanghai Ocean University, Shanghai, 201306, P. R. China*

[b]*College of Information, Shanghai Ocean University, Shanghai 201306, P. R. China*

E-mail addresses: 2629891285@qq.com (X. Cui), rlpei@shou.edu.cn (R. Pei)

*Corresponding author: zcwang1028@163.com (Z. Wang)

A novel combined VMD-MSMA-LSTM-ARIMA model for data-driven deep learning in precipitation prediction

Abstract: Accurate prediction of regional precipitation plays an important role in preventing natural disasters and protecting human life and property. In this study, the nonlinear monthly precipitation data are decomposed into multiple sub-signal intrinsic mode function (IMF) with different center frequencies based on variational modal decomposition (VMD) to mine multi-scale features. Then, a hybrid model built by long short-term memory (LSTM) and autoregressive integrated moving average model (ARIMA) is used to predict the residuals and IMFs. The hyperparameters such as the number of hidden layer nodes and training times of LSTM and the learning rate are optimized by using the modified smile mould algorithm (MSMA) based on the adaptive strategy and spiral search. This study also uses the model to predict precipitation in two regions. The empirical results show that VMD-MSMA-LSTM-ARIMA model perform better and the prediction is more accurate compared with others. The deep learning model established in this study can provide some reference for the accurate prediction of future precipitation in different regions.

Keywords: Precipitation prediction; Variational modal decomposition; Smile mould algorithm; Long and short-term memory; Autoregressive integrated moving average model

1 Introduction

Precipitation is the depth of water that falls on the ground at a certain point or over a certain area at a certain time. The difference of geographic space environment makes the precipitation in different areas have obvious variability. At the same time, global warming has become a problem that cannot be ignored under the action of human factors. In this context, analyzing and predicting

drought trends has an important role for disaster management (Zeng *et al.* 2022), because globally, droughts have the widest impact and cause the most severe economic losses. While the direct cause of droughts is the decrease of natural precipitation, the lagging management and dispatch of water resources due to the underestimation of precipitation is also an important factor in their disaster expansion. China is a drought-prone country with a wide drought area, which accounts for about 45% of China's land area. For example, the drought that occurred in China in 2009 affected 12 provinces and lasted for a long time and had a wide impact (Pradhan *et al.* 2017). Precise prediction of future precipitation in drought-stricken areas and advance drought response measures based on this is particularly important for China nowadays. In addition, due to the wide geographical area of China and the strong geographical characteristics of precipitation, the coexistence of droughts and floods in China is a frequent phenomenon. For example, in China, the average precipitation in 2020 increased by 10.3% compared to the normal year, and the rainy season lasted for a long time, with severe disasters such as heavy rainfall and flooding in the south in summer (Li *et al.* 2021). In recent years, unusual extreme weather has occurred, causing severe flooding events in different regions of China (Wu *et al.*2021). For instance, from July 17 to 23, 2021, Henan Province suffered from a rare historical extraordinarily heavy rainfall, with an average process rainfall of 223 mm in the province, far exceeding the historical extreme. This disaster was widespread and caused serious economic losses and casualties. Other examples are the largest autumn flood in the middle and lower reaches of the Yellow River since the same period in history in 2021, the continuous rainfall caused by the convergence of cold and warm air, the flooding in many places, and the heavy rainfall and flooding events in Shaanxi in the middle and late August, etc. This shows that the analysis of precipitation influencing factors and accurate rainfall prediction play an important role in the prevention of natural disasters such as droughts, floods and heavy rainfall. In addition, precipitation plays an irreplaceable role as an important regional source of water resources and a way of water circulation. With the development of the world economy and the expansion of population, the demand for water resources is increasing day by day, and water shortage is a common crisis faced by all mankind. Reasonable planning and allocation of water resources management and scheduling need to be based on the accurate prediction of regional precipitation. However, precipitation is a complex and dynamic process influenced by many factors and human activities, which is full of uncertainties and fluctuations, so

it is a challenging task to accurately predict regional precipitation.

2 Research progress

Currently, researchers have explored many models for precipitation prediction. Forecasting models for precipitation are broadly classified into three types (Adikari *et al.* 2021): the hydrological prediction method (Seo & Sung, 2020; Liang *et al.* 2019; Yang *et al.* 2020), the probabilistic statistical method (Van der Plas *et al.* 2017; Whan & Schmeits, 2018; Van Straaten *et al.* 2018) and time series methods (Papacharalampous *et al.* 2018; Yazdandoost *et al.* 2021; Wu & Wang, 2022; Alizadeh *et al.* 2022).

Hydrological phenomena occur due to the interaction of many inner and outer environmental factors. Hydrological prediction method based on the previous or current hydro-meteorological data, a certain area in a certain period of time in the future to make quantitative predictions of hydrological conditions. It is an approximate physical model derived from the generalization of complex hydrological phenomena and has an important role in the study of hydrological laws and the solution of practical problems in production. With the development of technology nowadays, the structure and methods of hydrological prediction models are being improved (Siddique *et al.* 2015; Al-Sabhan *et al.* 2003). Nowadays, different hydrological prediction models are proposed by research scholars, and precipitation prediction is receiving more and more attention as the main research direction of hydrological prediction. Brown *et al.* (2012) used a pooled hydrological model for joint forecasting of 10-20 hydrological basins. The study results showed that the model was more accurate for forecasting moderate precipitation than light or heavy precipitation. Dion *et al.* (2021) utilized eight set-total hydrological models and assimilated and updated them by using data from the ensemble kalman filter (EnKF) to provide the initial state to the model. Their findings show that the model can better sample uncertainties in hydrometeorological observations and reduce initial condition errors. Elsanabary *et al.* (2015) used the Sacramento Soil Moisture Accounting Model (SAC-SMA) of the US National Weather Service to simulate runoff in the Upper Blue Nile basin of Ethiopia. The outcomes of the study indicate that SAC -SMA performs better than a modified version of the Interactions Soil–Biosphere Atmosphere model (MISBA) in calibration runs and validation runs, and these results provide useful information on the impact of

global ocean anomalies on Upper Blue Nile Basin (UBNB) hydrology. Nowadays, distributed hydrological models are becoming a hot topic in precipitation prediction applications. Compared to integrated hydrologic models, distributed hydrologic models use mathematical equations that take into account spatial variations in input variables, hydrologic processes, binding conditions, and geometric features of the watershed, and the comprehensiveness of the model impact allows for more accurate predictions. Li *et al.* (2021) mentioned the use of a soil and vegetation model of distributed hydrology to simulate the Bresse River estuary watershed. The model combines spatial variability and hydrological processes and achieves good results. However, the application of hydrological model predictions is often based on the conditions of complete hydrological environment data, and the application of this type of models is greatly limited in unfamiliar environmental areas where data are lacking.

Probabilistic statistics, which is a mathematical model of stochastic systems using probability distributions and numerical characteristics of probability statistics, has also been widely used in precipitation prediction. Probabilistic prediction conveys the uncertainty and variability of rainfall prediction (Whan *et al.* 2018; Kumar *et al.* 2019), which is more in line with the fact that rainfall is susceptible to random disturbances in the external environment. One of the typical probabilistic statistical models is the Markov chain prediction method, proposed by Markov in the early 20th century. As a stochastic process theory, the nature of this model considers that the state at a given moment depends on the state at the previous moment and is independent of the system before the previous moment, which means that the influence of distant factors on the current state is very limited. Mahavarpour *et al.* (2014) developed a first-order two-state dry and wet frequency matrix using Markov chain model. Then, the transport probability matrix was established by the great likelihood method and the subsequent data of the selected model were determined by the cardinality superiority analysis, and by using this matrix, the stability probabilities and daily recurrence periods of rainfall and non-rainfall states in Iran were estimated. Tong *et al.* (2019) developed a Markov chain Monte Carlo prediction model for the complexity and stochasticity of precipitation series in Beijing, China. The results of the study showed that the Markov property was satisfied in the case of data at significance 0.1, and the prediction results were reliable. But Monte Carlo prediction is a method that applies random numbers to simulate experiments. The model samples the system with on-the-fly observations and achieves prediction of the system

based on the observation statistics of the sample values. Since the model requires the data series to obey a specific probability distribution, it has some application limitations. Simon *et al.* (2018) invented a probabilistic statistical method for predicting thunderstorms, which applies a generalized additive framework. The results showed that the prediction outperformed the predictions of climatological methods. However, probability statistics is not highly applicable to unsteady time series, and requires strong independence between model series data. But the application of probability statistics is limited by the coupling relationship between historical precipitation data and regional environmental factors, and the non-linear characteristics of precipitation such as obvious seasonality and periodicity. Thus, the method of prediction of nonlinear time series of precipitation has emerged.

Time series method, also known as trend forecasting method, is curve fitting or linear regression of time series, which is by far the most studied and popular quantitative forecasting method. It is based on the fact that the development process of things generally does not develop in leaps and bounds, but generally changes incrementally, and thus its future development changes can be inferred based on its historical trend. Nickerson *et al.* (2005) used the autoregressive integrated moving average model (ARIMA) to predict precipitation in east-central Florida and compared the nonlinear regression (NLR) and ARIMA model predictions for 1998 with the actual data for 1998. The results show the conclusion that the ARIMA model performs much better relative to the wet deposition values. The model was fitted using a mathematical function that requires a certain linear relationship for the precipitation series. Nevertheless, due to many intricate reasons precipitation series are mostly multi-scale series with a mixture of linear and nonlinear, and there are seasonal and unstable trends in precipitation, thus the ARIMA model, which deals mainly with linear data, cannot reflect the full characteristics of a comprehensive precipitation series. In contrast, artificial neural networks have autonomous learning ability and associative storage capability, which can fully approximate arbitrarily complex nonlinear relationships and have high robustness and fault tolerance. Haidar Ali & Verma Brijesh (2018) used deep convolutional neural networks (CNN) to predict monthly rainfall at selected locations in eastern Australia and compared it with the Australian Community Climate and Earth System Simulator Seasonal Prediction System (ACCESS), which showed that the proposed CNN prediction values are more accurate and have less error. Di Nunno *et al.* (2022) used two machine

learning algorithms, M5P and Support Vector Machine to predict precipitation in the northern part of Bangladesh with tropical monsoon climate, including Rangpur and Sylhet provinces, with good results. Kang *et al.* (2020) used a long short-term memory (LSTM) network model to predict precipitation in Jingdezhen city and compared the performance with other traditional machine learning algorithms. It was found that LSTM was suitable for precipitation prediction and the Recurrent Neural Network (RNN) model combined with meteorological variables increased the accuracy of model prediction. Meanwhile, the hyperparameters of the neural network model have a great influence on the prediction accuracy, and in the past, the selection of hyperparameters mostly chose default values or manual subjective estimation. With further research on precipitation prediction models, many scholars have used intelligent optimization algorithms to find the optimal parameters of neural networks and achieved good results. Lin *et al.* (2008) established a prediction model of genetic neural network and predicted short-term precipitation in Guangxi, and the results showed that the model overcame the randomness of the initial weights and avoided the problem of network oscillation and its getting into local solutions when determining the structure of neural network. Long *et al.* (2015) used particle swarm optimized wavelet multi-neural network for precipitation prediction, and the empirical results found that the accuracy of the prediction of the neural network based on genetic algorithm optimization is higher than that of the one without improvement. Jalalkamali *et al.* (2011) used genetic algorithm to optimize the hyperparameters of Artificial Neural Network (ANN), which makes the selection of hyperparameters of ANN automated and convenient, eliminating the error of human subjective selection. Zhang *et al.* (2022) mainly used artificial neural network based on back propagation of genetic algorithm to predict summer precipitation in the Yangtze River-Huaihe River basin in eastern China and compared with other models, and the results showed that the model has potential for summer precipitation forecasting.

In addition, although artificial neural networks can produce better simulation of precipitation, they do not essentially change the time series instability. If the original series is used directly as the input data, it will lead to the loss of some features. Toufan *et al.* (2015) decomposed the precipitation signal by selecting the mother wavelet and then predicted precipitation by fitting direct equation and Nero wavelet mixture for Zarringol station (Iran). The results show that the correlation between observed and calculated data is significantly improved by wavelet

decomposition of the signal, and the prediction accuracy is improved. It can be seen that the smoothing of data series or signals can be achieved by wavelet decomposition. But wavelet decomposition has the disadvantages of lack of adaptivity, the signal cannot meet the concentration in both time and frequency domains, the time accuracy and frequency accuracy cannot be satisfied at the same time, and the accuracy of dealing with sudden change signal is not high. Based on this, empirical mode decomposition (EMD) was introduced. Sun *et al.* (2014) predicted precipitation in northeast China based on radial basis function neural network (RBF) with EMD. The results show that the EMD-RBF model performs well in terms of prediction accuracy and provides a new method for precipitation forecasting. The EMD also has certain drawbacks, such as the existence of mode overlap, endpoint effect and difficult to determine the stopping condition. In order to overcome these drawbacks, variational modal decomposition (VMD) is proposed, which is a completely non-recursive frequency-based signal decomposition method. Compared with the time-frequency-based decomposition method of EMD, it greatly improves the efficiency of the algorithm, and VMD can achieve better separation of signals with similar frequencies, avoid the occurrence of modal overlap, and the decomposition results are more accurate. The VMD proposed by Dragomiretskiy & Zosso (2016) can decompose the nonlinear, unstable time series, search for the optimal solution of the variational modes through iterations, continuously update each mode function and the center frequency, and obtain several mode functions with certain broadband, which not only has strong robustness but also can effectively avoid the modal mixing phenomenon. Therefore, the accuracy of precipitation time prediction can be improved. Li *et al.* (2020) developed a combined VMD, least squares support vector machine (LSSVM), adaptive Volterra, improved butterfly optimization algorithm (IBOA), and Auto-Regressive and Moving Average Model (ARMA) for precipitation forecasting at two stations in Shanxi Province, China. The results show that the model can effectively reduce the precipitation forecast errors.

In recent years, the impact of human activities and changes in the form of the regional water cycle have greatly influenced the prediction models in the temporal and spatial dimensions of precipitation influences (Dikshit & Pradhan 2021; Ilyés *et al.*2021; Zhang *et al.* 2020), making the accurate prediction of precipitation a major challenge. Moreover, precipitation time series are actually superimposed series formed by linear and nonlinear series, and it is inappropriate for

previous analyses to classify precipitation series into one of these categories for prediction in a one-sided manner. To further improve the precipitation prediction accuracy, this study proposes a combined model based on VMD-MSMA-LSTM-ARIMA. Spectral decomposition with VMD is used to obtain eigenmodal sequences with the same frequency characteristics, reducing the adverse effects caused by ground modal mixing due to the original single sequence state. Then the LSTM and ARIMA models are combined to take advantage of their respective strengths in dealing with nonlinear and linear series, each complementing the other. the ARIMA model performs linear prediction on the decomposed modal series of VMD, and then inputs the difference into the LSTM model for nonlinear prediction. The LSTM hyperparameters are also optimized using the modified slime mould algorithm (MSMA) to enhance the prediction accuracy.

3 Research progress

3.1 Variational Modal Decomposition

VMD is a completely non-recursive signal processing method that allows filtering of nonlinear time series (Carvalho *et al.*, 2021).VMD determines the number of given modal decompositions according to the actual situation, achieves the effective segregation of intrinsic modal fractions (IMFs) by matching the optimal center frequency and the preferred width, and then obtains the effective decomposition components of the given signal, and finally obtains the variational The optimal solution of the problem is obtained. Furthermore, it can be seen that the center frequency-based feature extraction method has good separability (Yang & Zhang, 2016). Its steps are as follows:

(1) The analytic signal obtained $v_k(t)$ by Hilbert transform is calculated so that the center band of the analytic signal is modulated to the corresponding baseband as shown in Eq. (1):

$$\left[\left(\delta(t)+\frac{j}{\pi t}\right)v_k(t)\right]e^{-jwkt} \tag{1}$$

In Eq. (1): $\delta(t)$ is the Dirac function and $v_k(t)$ is the convolutional function.

(2) The bandwidth of each subseries is estimated by calculating the squared parametrization

of the demodulation gradient. The subsequence is a modal component with a finite bandwidth at the center frequency, while the sum of the estimated bandwidths of each mode is minimized and the sum of all modes is equal to the original signal. The corresponding constrained variational expression is shown in Eq. (2):

$$\begin{cases} \min\limits_{\{v_k\}\{w_k\}} \left\{ \sum\limits_{k=1}^{k} \| \partial_t \left[\left(\delta(t) + \frac{j}{\pi t} \right) v_k(t) \right] e^{-jw_k t} \|^2 \right\} \\ s.t. \sum\limits_{k=1}^{k} v_k(t) = s \end{cases} \tag{2}$$

In Eq. (2): k is the number of modes to be decomposed (positive integer), v_k, w_k corresponds to the k-th mode variable and the central frequency after decomposition, respectively.

In order to find the optimal solution, VMD introduces the Lagrange multiplier operator $\tau(t)$ and the second-order penalty factor α to transform the constrained variational problem into an unconstrained variational problem. Among them, the second-order penalty factor $\tau(t)$ can ensure the accuracy of signal reconstruction in Gaussian noise environment, and the Lagrange multiplier operator α can maintain the strictness of the constraints. The augmented Lagrangian expression is Eq. (3):

$$L\left(\{v_k\},\{w_k\},\tau\right) = \alpha \sum_{k=1}^{k} \| \partial_t \left[\left(\delta(t) + \frac{j}{\pi t} \right) v_k(t) \right] e^{-fwkt} \|_2^2 + \| s(t) - \sum_{k=1}^{k} v_k(t) \|_2^2 + \left\langle \tau(t), s(t) - \sum_{k=1}^{k} v_k(t) \right\rangle \tag{3}$$

(3) Using the Alternating Direction Method of Multipliers (ADMM) iterative algorithm combined with Fourier isometric variation, the optimization waits for each modal component and the center frequency, and searches for the saddle point of the extended Lagrangian function. The expression after the alternating optimization-seeking iteration is Eq. (4):

(4)

In Eq. (4): $\hat{v}_k^{n+1}$, $\hat{s}(\omega)$, $\hat{\tau}(\omega)$ correspond to the Fourier transform of $v_k^n(t)$, $s(t)$, $\tau(t)$ respectively.

(4) to the residual after Wiener filtering, the algorithm re-estimates the center of gravity

frequency as the process follows:

①Initialize $\hat{v}_k^1$, $\hat{\omega}_k^1$, $\hat{\tau}_k^1$ and n.

②Execution of the next cycle $n+1 \longrightarrow n$.

③At that time, update ω_k as in Eq. (5):

$$\omega_k^{n+1} = \frac{\int_0^\infty \omega |v_k^{n+1}(\omega)|^2 d\omega}{\int_0^\infty |v_k^{n+1}(\omega)|^2 d\omega} \tag{5}$$

④Update $\hat{\tau}$ as in Eq. (6):

(6)

⑤Repeat steps ② to ⑤ until the iteration condition is satisfied as shown in Eq. (7):

(7)

3.2 Long short-term memory neural network

LSTM is a special type of recurrent neural network capable of capturing long-time dependencies and is commonly used to process and predict events with long intervals and delays in time series (Gers *et al.* 2002) for solving the gradient disappearance problem during training of long sequences. In many studies table LSTM outperforms traditional recurrent neural networks in the prediction of time series. LSTM consists of multiple memory cells. To control the long-term cell states, the LSTM model uses a gate structure, where each cell has an oblivion gate, an input gate and an output gate, and the LSTM memory cells have a long and short-term memory mechanism. The gate structure is a way to let information pass through selectively. the network structure of LSTM is shown in **Fig. 1**. It can be seen from the figure that the LSTM has three inputs and two outputs at moment *t*. The structural system of the LSTM model is as follows:

(1) Forgetting gate, which is mainly used to determine how much information about the

previous cell states should be remembered by the current model. Based on the sigmoid function to retain or forget the content of previous cell states. sigmoid function layer output between 0 and 1 is used to indicate how much information should pass through for each component. A zero means that no messages can pass, while a one means that all messages can pass. Historical information that can indicate long-term trends is filtered and saved, and non-critical information is discarded. The forgetting gate f_t formula is shown in Eq. (8):

$$f_t = \sigma\left(W_{rf}s_{t-1} + W_{xf}x_t + W_{cf}c_{t-1} + b_f\right) \tag{8}$$

In Eq. (8): W and b_f are the weight matrix and bias value of the forgetting gate, respectively.

(2) Input gate, the input gate updates the current cell state by adding the product of the output of the forgotten gate and the previous cell state to the product of the output of the input gate and the input activation. The input gate i_t and the cell state update equation c_t are shown in Eqs. (9) - (10):

$$i_t = \sigma\left(W_{ri}h_{t-1} + W_{ri}x_t + W_{ci}c_{t-1} + b_i\right) \tag{9}$$

$$c_t = f_t c_{t-1} + i_t \sigma\left(W_{rc}h_{t-1} + W_{xc}x_t + b_c\right) \tag{10}$$

In Eqs. (9) - (10): σ is the activation function, W is the weight matrix; b is the bias value of the corresponding gate, and c_t is the cell state output after this cell is updated.

(3) Output gates, which output the results of the LSTM model for that layer to the LSTM at the next time step in order to pass the history information to the next block. The output gate is determined by the part of the study that wants to output the cell state. The formula for calculating the output value o_t of the output gate using the equation is shown in Eq. (11):

$$o_t = \sigma\left(W_{ro}h_{t-1} + W_{xo}x_t + W_{co}c_{t-1} + b_o\right) \tag{11}$$

Finally, the output at moment t is shown in Eq. (12):

$$h_t = o_t \tanh\left(c_t\right) \tag{12}$$

In Eqs. (11) - (12): at the current time t, x_t denotes the input, h_{t-1} denotes the output at the previous moment, c_{t-1} denotes the hidden state at the previous moment, the current LSTM value

is c_t, and the output value is h_t.

Fig. 1 is near here.

3.3 Slime Mould Algorithm

3.3.1 Principle of slime mould algorithm

The slime mould algorithm (SMA) is an algorithm inspired by the movement of slime bacteria (Houssein *et al.* 2021), which uses a mathematical model to imitate the behavior and shape changes of slime bacteria foraging. The slime bacteria foraging process generally has the following three stages. first is the approaching food stage, followed by the encircling food stage. The mathematical model of this stage is built on the basis of simulated mucilage tissue venous contraction pattern, the mucilage approaches the food according to the food odor. The higher the odor concentration, the stronger the bio-oscillator wave, the faster the cytoplasm flow, the thicker the mucilage venous-like tube. Finally, there is the food acquisition stage, in which the mucilage still has a certain probability of searching unknown areas. The behavior of this slime bacterium approximation is simulated by functional expressions, and its behavior is expressed by Eqs. (13) - (14):

$$X(t+1)=\begin{cases} rand.(UB-LB)+LB & rand<z \\ X_b(t)+vb.(W.X_A(t)-X_B(t)) & r<p \\ vc.X(t) & r\geq p \end{cases} \tag{13}$$

$$p=\tanh|S(i)-DF| \tag{14}$$

In Eqs. (13) - (14): $X_{(t+1)}$ and $X_{(t)}$ represent mucilage locations, $X_b(t)$ represents the t-th best location, X_A and X_B are two randomly selected mucilage locations, vc decreases linearly from 1 to 0, a is shown in Eq. (15):

$$a=\arctan h\left(-\frac{1}{\max T}+1\right) \tag{15}$$

In Eq. (15): max$T$ denotes the maximum number of iterations. W is the weight of the mucilage, expressed in the form shown in Eqs. (16) - (17):

$$W\left(SmellIndex(i)\right)=\begin{cases}1+r.\log\left(\dfrac{bF-S(i)}{bF-\omega F}+1\right), condition\\ 1-r.\log\left(\dfrac{bF-S(i)}{bF-\omega F}+1\right), others\end{cases} \tag{16}$$

$$smellIndex=sort\left(S\right) \tag{17}$$

In Eqs. (16) - (17): *condition* simulates the process of adjusting the position of slime bacteria according to the food concentration, denotes the population with $S(i)$ ranked in the top half, *r* is a random number from 0 to 1, *bF* denotes the optimal fitness during the current iteration, denotes the worst fitness value during the current iteration, and *smellIndex* denotes the fitness sequence.

3.3.2 Modified slime mould algorithm

In the slime mould algorithm (SMA), the parameter a plays an important role in the global exploration and local exploitation ability of the algorithm, the initial parameter a decreases faster in the early iterations, and a smaller parameter a is not conducive to global search (Tang *et al.* 2021). Therefore, to improve the global exploration capability and the convergence capability of local development, this study proposes a new nonlinear decreasing strategy with a new definition formula of parameter a as Eq. (18) is shown as follows:

$$a=2.75-2.75\left[1/\left(1+e^{-8(t/T_{\max}-0.5)}\right)\right] \tag{18}$$

In Eq. (18): t is the current number of iterations, $T\max$ is the maximum number of iterations.

The adaptive adjusted parameter a maintains a larger weight at a smaller rate in the early iteration to effectively slow down the early iteration, increase the global exploration time and improve the global search capability. **Fig. 2** shows the change process of parameter a during the iteration process, from the figure, we can visually represent the comparison of the early decline speed and the size of parameter a taken before and after the improvement.

Fig. 2 is near here.

In order to enhance the ability to explore unknown regions and improve the global search

capability of the sticky bacterium optimization algorithm, inspired by the whale optimization algorithm (WOA), this study incorporated the spiral optimization search strategy into the SMA (Samantaray & Sahoo.2021). The mathematical model of whale hunting behavior is shown in Eqs. (19) - (20):

$$X\left(t+1\right)=X_b\left(t\right)+e^l\cos\left(2\pi l\right)\left(X_b\left(t\right)-X\left(t\right)\right) \tag{19}$$

$$l=1-2\left(\frac{t}{T\max}\right) \tag{20}$$

In Eqs. (19) - (20): $X_b(t)$ may be the location of the current optimal solution may also be a random search unit location, l is a random value, the range of values for [-1,1].

Experimental validation was conducted to compare the selected parameters for the locations, and it was found that the precipitation prediction was more accurate for the two areas under the selected parameters, so on this study, the selected location update position is shown in Eq. (21):

$$X(t+1)=\begin{cases} rand.\left(UB-LB\right)+LB, & r<z \\ X_b(t)+vb.\left(W.X_A(t)-X_B(t)\right), & r<p\,\&\,r<0.87 \\ X_b(t)+e^l\cos\left(2\pi l\right)\left(X_b(t)-X(t)\right), & r<p\,\&\,r\geq 0.87 \\ vc.X(t), & r\geq p\,\&\,r<0.13 \\ X_b(t)+e^l\cos\left(2\pi l\right)\left(X_b(t)-X(t)\right), & r\geq p\,\&\,r\geq 0.13 \end{cases} \tag{21}$$

Compared to the previous location update formulas, the updated search improvement formula is more refined in the confirmation of location, allowing for an increased search range for the space. The slime individuals will search in the search space in the form of spirals, extending the ability of slime individuals to explore unknown regions. This will make it more likely for the algorithm to jump out of the local optimum and effectively improve the global search performance of the algorithm. In this study, the slime mould algorithm modified by adaptive parameter adjustment and spiral search strategy is called MSMA.

3.4 Autoregressive Integrated Moving Average model

Box and Jenkins proposed the Autoregressive Integrated Moving Average Model (ARIMA) in

1970. This model is a time domain model used to fit linear time series (Lai & Dzombak. 2020). ARIMA (*p, d, q*) in AR is autoregressive, MA is the moving average, *p* is the autoregressive term, *q* is the moving average term, and *d* is the number of differences made to make it a smooth series. The model can transform non-linear time series into linear time series for mathematical fitting, and the ARIMA model has the following three steps:

(1) Smoothing test to determine the value of *d*

The ADF test is performed on the time series to see if the series is smooth. A d-order difference is performed for non-stationary series to make it a smooth time series.

(2) Autoregressive model (AR) and moving average (MA)

For the smooth series, the order is generally determined by first applying the partial autocorrelation coefficient (PAC) and the autocorrelation coefficient (ACF) in the initial determination of the order *p* and *q* of the ARIMA model, and then finalized by the Akaike Information Criterion (AIC).

(3) Model prediction

The defining equations of the ARIMA model are shown in Eqs. (22) - (23):

$$y_t = \alpha + \varepsilon_t + \sum_{i=1}^{p} \theta_i y_{t-1} + \sum_{i=1}^{q} \phi_i \varepsilon_{t-i} \tag{22}$$

$$\theta(B) y_t = \alpha + \phi(B) \varepsilon_t \tag{23}$$

In Eqs. (22) - (23):y_t denotes the value at the current time; θ_i denotes the AR coefficient of order *p*; φ_i denotes the MA coefficient of order *q*; α is the constant term; ε_t denotes the error term, and *B* denotes the backward shift operator. For non-smooth series, the difference operator ∇^d is used. where the formula for ∇^d is shown in Eq. (24):

$$\Theta B = \nabla^d = (1-B)^d \tag{24}$$

The final ARIMA (*p*, *d*, *q*) model can be written in the form of Eq. (25):

$$\theta(B)\Theta(B) y_t = \alpha + \varphi(B) \varepsilon_t \tag{25}$$

3.5 Precipitation prediction model based on VMD -MSMA -LSTM-ARIMA

For precipitation time series data with uncertainty and complexity, the prediction model proposed in this study is divided into three main stages (Wang *et al.* 2021): Firstly, the variational modal decomposition method is used to decompose the precipitation into smooth modal components at different frequency dimensions. Secondly, the ARIMA model, the most well-known linear statistical model, can capture linear trends very well (Fan *et al.* 2021), while the LSTM model can accurately describe the nonlinear trend because of its unique structure, and the hybrid model of the two can complement each other to predict the precipitation data more accurately. Therefore, IMF1, IMF2, IMF3, ..., IMFn and the residuals (the difference between the modal components and the original series after VMD decomposition) from high frequency to low frequency are imported into the ARIMA model for prediction, and the output of ARIMA is used as the input of the LSTM model. Since the hyperparameters of the LSTM cannot be matched with the precipitation data effectively, and the hyperparameters of the LSTM have a large impact on the model prediction, this study will optimize the number of hidden layers, the learning rate, and the maximum number of iterations of the LSTM based on the adaptive strategy and the improved spiral search of the viscous bacteria optimization algorithm to obtain the optimal parameter values and then construct the model, and use the corresponding subseries data to train the network. Training is performed using the corresponding subsequence data. The trained network is then used to predict the sub-sequences. Finally, each IMF subseries' predictions and residuals are summed. **Fig. 3** shows the flow of the model proposed in this study.

Fig. 3 is near here.

The VMD-MAMA-LSTM-ARIMA model is detailed as follows:

(1) The preprocessed data series are decomposed into modal components, and the original data are decomposed into IMF1, IMF2, IMF3, ..., IMFn and the residuals (the difference between each modal component and the original sequence) are noted as Residual.

(2) Denote IMF1, IMF2, IMF3, ..., IMFn are denoted as Y_i (i=1, 2, 3, ..., n) and Residual (Y_{i+1}) are imported into the ARIMA model, respectively, and the smoothness test as well as the

model sizing are performed for each component to obtain the predicted values L_t.

(3) Calculate e_t (nonlinear time series) and use Y_t-L_t as input to the lstm model. Normalize the experimental data and divide the training set and test set.

(4) Initialize the improved SMA algorithm (number of populations, number of iterations, etc.) and use the number of hidden layers, learning rate, and maximum number of iterations of the LSTM as optimization parameters.

(5) Set the sticky bacteria speed, sticky bacteria fitness value, update the iterations, find the best position, and use its optimal solution as the hyperparameter value of the LSTM.

(6) The model is trained and the test set is predicted to get the prediction results for each set.

(7) The sub-test sets as well as the residual test sets are superimposed to get the final prediction results.

3.6 Model prediction accuracy evaluation index

The error rating indices used in this study are mean absolute percentage error (MAPE), root mean square error (RMSE), mean absolute error (MAE) and coefficient of determination (R^2), nash-sutcliffe efficiency coefficient (NSE), NSE is generally used to verify the goodness of the hydrological model simulation results. The conditions for evaluating the merits of the model are RMSE, MAE, MAPE must be minimum and must be maximum, The NSE is near 1, which means that the model has good prediction effect and high credibility; the NSE is near 0, which means that the simulation results are roughly plausible, but the procedure modelling error is large; the NSE is much less than 0, which means that the model is not credible. The evaluation indicators are shown in Eqs. (26) - (30):

$$RMSE=\sqrt{\frac{1}{N}\sum_{i=1}^{N}\left[X_f(i)-X_o(i)\right]^2} \tag{26}$$

$$MAPE=\frac{1}{N}\sum_{i=1}^{N}\left|\frac{X_o(i)-X_f(i)}{X_o(i)}\right| \tag{27}$$

$$MAE=\frac{1}{N}\sum_{i=1}^{N}\left|X_f(i)-X_o(i)\right|$$

(28)

$$R^2 = \frac{\left\{\sum_{i=1}^{N}\left[X_o(i)-\overline{X}_o\right]\left[X_f(i)-\overline{X}_f\right]\right\}^2}{\sum_{i=1}^{N}\left[X_o(i)-\overline{X}_o\right]^2\sum_{i=1}^{N}\left[X_f(i)-\overline{X}_f\right]^2}$$

(29)

$$NSE = 1-\frac{\sum_{i=1}^{n}(X_o(i)-X_f(i))^2}{\sum_{i=1}^{n}(X_o(i)-\overline{X}_o)^2}$$

(30)

In Eqs. (26) - (30): N is the number of forecast months; $X_f(i)$ is the predicted precipitation; $X_o(i)$ is the measured precipitation; $\bar{X}_o$ is the average value of measured runoff; $\bar{X}_f$ is the average value of predicted runoff.

The prediction interval coverage percentage (*PICP*) and the Mean prediction interval (*MPI*) are also used in this study to evaluate the prediction reliability and model uncertainty of the developed data-driven model. The prediction interval (*PI*) is the range of values that may be obtained for the next observation and indicates the threshold for accepting or rejecting the predicted value. *PICP* indicates how often the actual observation falls within the prediction interval, which is used to determine the reliability of the predicted value. *MPI* is the average width of the prediction interval, which is the average distance between the upper limit of the prediction interval PI_i^{up} and the lower limit of the prediction PI_i^{low}. The indicators are shown in Eqs. (31) - (35):

$$s = \sqrt{\frac{\sum_{i=1}^{N}\left(\hat{y}_i - y\right)^2}{n-1}}$$

(31)

$$PI_i^{up} = \hat{y}_i + t_{n-p}^{\alpha/2}s$$

(32)

$$PI_i^{low} = \hat{y}_i - t_{n-p}^{\alpha/2}s$$

(33)

$$PICP = \frac{1}{n}\sum_{i=1}^{n}c_i$$

(34)

$$MPI = \frac{1}{n}\sum_{i=1}^{n}(PI_i^{up} - PI_i^{low})$$

(35)

In Eqs. (31) - (35): s is the standard deviation of the model prediction. PI_i^{up} is the upper limit of the prediction interval corresponding to the *i-th* observation, and PI_i^{low} is the lower limit of its prediction interval. PI_i is the prediction interval of the developed prediction model for the precipitation time series; $t_{n-p}^{\alpha/2}$ is the t-distribution with $n-p$ degrees of freedom for $(1-\alpha)\%$. If the predicted values obey a normal distribution, $t_{n-p}^{\alpha/2}$ is 1.96 at 95% confidence interval.$c_i = 1$ is the judgment coefficient if y_i lies in the prediction interval, otherwise $c_i = 0$. This study considers that if $PICP \geq 95\%$, then its predictive value is assumed to be reliable.

In addition, the standard deviation (SD) and root mean square error (RMSE) between the predicted and measured values of the model and the coefficient of determination (R^2) were also investigated in this study using Taylor plots.

4 Empirical analysis of the model

4.1 Introduction of data sources

This study selected monthly precipitation data from January 1951 to December 2021 in Ankang City, Shaanxi Province, China, for a total of 824 groups. In Ankang City, deep in the inland hinterland of northwest China, it has a subtropical continental monsoon climate with obvious differences in precipitation between the four seasons, with cold and little rain in winter, warm and dry and also less precipitation in spring, but prone to short-duration rainstorms in summer and autumn. In addition, the area is located in the Loess Plateau area, the average annual precipitation is low and the local agricultural water use is mainly based on natural precipitation. Therefore, precipitation prediction for the Ankang City will be of great significance for the rational arrangement of agricultural production. To verify the wide applicability of the model in different geospatial environments, 867 sets of monthly precipitation data from January 1951 to March 2022 in Yongding District, Longyan City, Fujian Province, China, were also selected as samples in this

study. Yongding District is located in the southeast coast of China, with a subtropical maritime monsoon climate, warm and humid, and an average rainfall of 1400-2000 mm, which is one of the richest provinces in China in terms of annual precipitation, far exceeding that of Ankang City. The rivers in Yongding District are all mountainous and stormy rivers, which are greatly influenced by topography and climate, with rapid and swift water flow. Accurate prediction of precipitation can help prevent and mitigate floods and protect life and property in the area. The geographical location information of Ankang City and Yongding District is shown in **Fig. 4**, and the precipitation statistics of the two areas are shown in **Table 1**. In both groups, we selected 90% as the training set data and the remaining as the validation set data, and the research data are shown in **Fig. 5**.

Table 1 is near here.

Fig. 4 is near here.

Fig. 5 is near here.

4.2 Selection of other LSTM hyperparameters

After optimizing the learning rate, the number of hidden layers and the maximum number of iterations with the genetic algorithm, we selected the optimizer, activation function and batch size of LSTM, and conducted a comparative analysis on the evaluation indexes of time and prediction results, in order to find the initial value of the hyperparameters suitable for this study. Because the LSTM is random, the evaluation index is obtained by calculating the average value after 20 runs. Using Ankang precipitation as raw data. **Table 2** shows the influence of activation function selection on results under the condition that other conditions are the same. It can be seen from the table that under the condition that activation function selection Sigmoid and tanh, the time is less and the error is smaller; **Table 3** shows the influence of optimizer selection and batch size selection on results under the condition that other conditions are the same. Under the condition that optimizer selection Rmsprop, the error evaluation is smaller and the time is faster. Larger batches usually lead to faster convergence of the model, but may result in a less optimal final set of weights. The batch size is the number of samples between updates of the model weights, If the

batch size is about 20-30, the error value is smaller. The batch size is too large, although the time will be reduced, but the error value will increase with it, so in the subsequent study the batch size is chosen to be 25. Run the results into the model predictions.

Table 2 is near here.

Table 3 is near here.

4.3 VMD model

The LSTM and ARIMA models cannot effectively handle the non-stationary ground precipitation data, so VMD counts are first used to decompose the precipitation. When decomposing by variational module, the value of modal number k has a great influence on VMD decomposition, and improper selection will cause large errors. k value can be decided by the central frequency, and the latest frequency is relatively stable then the optimal modal number. After experimental testing of the algorithm, the optimal number of modes for precipitation prediction in Ankang City, Shaanxi Province is 6, while the optimal number of modes for Yongding District, Fujian Province is 12. **Figs. 6** and **7** show each IMF component for Ankang City and Yongding District. The decomposed sub-series show the trend of the original precipitation series, periodization and other characteristics, so the prediction of each component can be effectively improved. **Fig. 8** shows the comparison of the results with and without VMD decomposition in the prediction model. Since the LSTM is random, the metrics are averaged after 20 runs, as is the case below. From the results, it is found that the values of error indicators MAPE, MAE, and RMSE are reduced after the VMD decomposition, indicating that the VMD method can effectively remove the non-smoothness associated with the original series. Next, we will demonstrate the superiority of VMD by comparing it with other decomposition models, starting with the more frequently used EMD, however, nowadays, on the basis of EMD, many superior decomposition methods are produced, such as ensemble empirical mode decomposition (EEMD), complementary ensemble empirical

mode decomposition (CEEMDAN), EEMD utilizes the statistical properties of EMD filter bank behavior and uniform distribution of white noise spectrum to make the distribution of signal polar points more uniform during filtering, and effectively suppress the interference caused by intermittent high frequency components, etc. Modal aliasing, CEEMDAN adds positive and negative paired auxiliary white noise to the original signal, and phase elimination at ensemble averaging, which can effectively improve the decomposition efficiency and overcome the problems of large reconstruction errors and poor decomposition completeness of EEMD. As shown in **Fig. 9** for the comparison of prediction errors for VMD, EMD, EEMD, and CEEMD combined with the LSTM model, it can be seen from the figure that VMD has the smallest value of the three errors, which shows that VMD has the advantage in precipitation prediction, and, as can be seen in the figure that the prediction accuracy of VMD has been significantly improved relative to EMD, indicating that VMD has some advantages over other decomposition models. EMD can decompose the original sequence data adaptively without pre-set parameters, while in VMD, the noise tolerance is set to 0, the tolerance of the convergence criterion is set to 1e-7, and the medium bandwidth constraint is set to 1000 by default. Compared with Compared with EMD, the IMFs decomposed by the VMD method all have independent central frequencies and exhibit sparsity in the frequency domain, with the qualities of sparse studies. However, EMD's high-frequency fractions are concentrated in the first few fractions, which can easily lead to modal mixtures. And in the process of solving the IMF, the endpoint effect similar to that in the EMD decomposition is avoided by the mirror extension.

Fig. 6 is near here.

Fig. 7 is near here.

Fig. 8 is near here.

Fig. 9 is near here.

4.4 ARIMA model

Each IMF component as well as the residuals were subjected to a smoothness test (Zhang *et al.* 2022) , and **Tables 4** and **5** show the ADF test tables for the two regions, from which it is seen that no unit root was detected in the ADF test at 1%, 5%, and 10% significance levels, proving that the

decomposed components are all smooth and therefore the IMF can be modeled, with p, q values derived from the autocorrelation and partial autocorrelation coefficients, as well as the AIC and BIC criteria. In the prediction process, since the LSTM is randomized, the predicted values are averaged after running 20 groups and analyzed. **Fig. 10** shows the comparison of the error evaluation metrics of the model with and without ARIMA and the model prediction results. The figure shows that all other conditions being the same, all three error ratings decrease, indicating that the addition of the ARIMA model has a better fit to the linear part of the precipitation time series and has a higher predictive accuracy than the LSTM model alone.

Table 4 is near here.

Table 5 is near here.

Fig. 10 is near here.

4.5 Comparison of genetic algorithms

We chose to evaluate the performance of a genetic algorithm using a set of benchmark mathematical functions. The benchmark mathematical functions are shown in **Table 6**. To demonstrate the superiority of SMA, we chose some test functions for unimodal (f1, f2) and multimodal (f3, f4) standard benchmarks, which are listed in **Table 7**. The unimodal functions have only one global optimum and no local optimum, so they are suitable for benchmarking the algorithm, while the multimodal functions have multiple local optima, so they help to test the global search ability of the genetic algorithm.

Table 6 is near here.

Table 7 is near here.

To verify the performance of SMA, we selected the popular algorithms summarized in **Table 7** and optimized the test functions in **Table 6.** For each algorithm, 30 search agents were used and 1500 iterations were performed. The relevant parameters for the parametric algorithms in question are shown in **Table 7**. The convergence curves for 1500 iterations of each function are summarized in **Fig. 11**, with each subplot representing a test function. It can be seen from the plots that SMA can find better solutions than other algorithms and has a shorter running time, thus

indicating that SMA has better global search capability and faster convergence. In addition, the results of the runs of the functions (f1, f2, f3 and f4) are listed from **Table 8**, thus reflecting the SMA performance. In terms of convergence values, SMA can search for more accurate values compared to other algorithms. In terms of running time, SMA is slower than WOA and MFO, but the difference is not significant, but the convergence speed is much faster than the other algorithms. Therefore, based on its excellent performance, SMA is applied to precipitation prediction.

Fig. 11 is near here.

Table 8 is near here.

4.6 Impact of the MSMA optimization algorithm

When ARIMA and LSTM are used to build the prediction models, the key parameters of LSTM model such as hidden layers, hidden nodes, learning rate and other key parameters are the key to improve the prediction effect of LSTM model. In this study, we set the number of hidden layers, learning rate and training times of LSTM model as the hyperparameters to be optimized, and use MSMA to automatically calibrate the above hyperparameters of LSTM. The interaction with the LSTM during the evolution of the slime population improves the prediction accuracy of the LSTM model. The initial range of values for each hyperparameter was obtained by combining the experimental tests as follows, the range of the number of hidden layers [200,400], the number of training iterations [200,500], and the range of values for the learning rate [0.01,0.001]. The number of populations of slime bacteria is set to 30, the maximum number of iterations is 500, and the position update parameter takes the value of 0.03. In the prediction process, since both LSTM and genetic algorithms are randomized, the predicted values are averaged after running 20 groups and analyzed. **Fig. 12** shows the comparison of the error indicator values after model prediction by different intelligent optimization algorithms. The MAE, MAPE, and RMSE index values decreased after MSMA than after SMA, especially the MAPE index value decreased from 2.0635 to 0.6615, a decrease of 67.9%, indicating that the improved SMA is more accurate for hyperparameter search, and the global search capability is greatly improved, which enhances the accuracy of model prediction. And compared with other optimization algorithms such as MFO and

WOA, MSMA also has a greater advantage, which fully illustrates that MSMA brings optimization effect to the LSTM model.

Fig. 12 is near here.

4.7 Comparative analysis

To better reflect the strengths and weaknesses of the modalities, the error ratings obtained from the other seven models are compared. **Tables 9** and **10** show the error assessment values of precipitation prediction for each model in Ankang City, Shaanxi and Yongding District, Fujian. From the tables, it can see that VMD-MSMA-LSTM -ARIMA is always the best among all the indicators, which proves that the model is more helpful for monthly precipitation prediction, and the NSE value is close to 1, which proves that the model is of good quality and high reliability. **Figs. 13** and **14** show the linear fit of each model in the two regions, from which it can be seen that the improved model R^2 is closer to 1 and the prediction results are more accurate. **Fig. 15** shows the Taylor diagram of the model for predicting precipitation series in Ankang City, Shaanxi Province. From the figure, it can be seen that according to the values of standard deviation (SD), R^2, and RSME, VMD-MSMA-LSTM-ARIMA is the closest model to the observed values, and it is clear from the data that the VMD-MSMA-LSTM-ARIMA model has better precipitation prediction capability. **Figs. 16** and **17** show the error intervals of the predictions of the two regions by different models. From the figures, it is concluded that the errors of the improved models are concentrated in the central interval, and the errors are mostly concentrated in the interval [-4,4], VMD-MSMA-LSTM-ARIMA, VMD-MSMA-LSTM, VMD-SMA-LSTM, VMD-MFO-LSTM, VMD-WOA-LSTM, VMD-LSTM, SMA-LSTM, LSTM for Ankang precipitation errors in the interval are 59.76%, 53.66%, 23.17%, 42.68%, 48.78%, 46.34%, 10.96%, 15.85%, and for Yongding precipitation errors in the interval are 61.63%, 46.51%, 50%, 46.85%, respectively. 46.51%, 50%, 46.51%, 46.51%, 52.33%, 2.33%, and 4.65%, respectively. Among them, the probability distribution density of VMD-MSMA-LSTM-ARIMA in this interval is much higher than other models, which indicates that this model has the least prediction error. The prediction curves of the different models for the monthly precipitation series of the two regions are shown in **Figs. 18** and **19**. After detailed observation, the predicted values by the

VMD-MSMA-LSTM-ARIMA model are closer to the actual values, and the predicted values fall within the 95% confidence interval the most, and **Figs. 20** and **21** show the predicted values by the VMD-SMA-LSTM-ARIMA model, and the prediction interval coverage (*PICP*) criterion, it can be seen that the model achieves *PICP* values of 98.78% and 100% for the predicted values of the two sites, which proves that the results are extremely reliable. **Fig. 22** shows the box plots of the predicted precipitation values for Ankang City and Yongding District based on the eight models. As can be seen from the figure, there is a high degree of match between the original data and the predicted values of the VMD-MSMA-LSTM-ARIMA model, and it can be visualized that the distribution characteristics of the original data and the predicted values of the VMD-MSMA-LSTM-ARIMA model are approximately the same. For Ankang City, the maximum value of the original data is 216.8 mm, and the VMD-MSMA-LSTM-ARIMA, VMD-MSMA-LSTM, VMD-SMA-LSTM, VMD-MFO-LSTM, VMD-WOA-LSTM, VMD-LSTM, SMA-LSTM, LSTM are 215.31 mm, 218.78mm, 225.62mm, 215.99mm, 209.64mm, 210.05mm, 157.24mm, 146.72mm, respectively, as can be seen. For Yongding District, the upper quadrant of the original data is 185.41mm, VMD-MSMA-LSTM-ARIMA, VMD-MSMA-LSTM, VMD-SMA-LSTM, VMD-MFO-LSTM, VMD-WOA-LSTM, VMD-LSTM, SMA-LSTM, LSTM are 183.45mm, 182.16mm, 183.28mm, 179.88mm, 182.56mm, 181.66mm, 181.24mm, 178.64mm, and the difference between the upper and lower edges of the original data is 376.58mm, VMD-MSMA-LSTM-ARIMA, VMD-MSMA-LSTM, VMD-SMA-LSTM, VMD-MFO-LSTM, VMD-WOA-LSTM, VMD-LSTM, SMA-LSTM, LSTM are 378.4mm, 379.39mm, 376.26mm, 376.64mm, 372.44mm, 373.44mm, 271.48mm, 241.08mm.

Table 9 is near here.

Table 10 is near here.

Fig. 13 is near here.

Fig. 14 is near here.

Fig. 15 is near here.

Fig. 16 is near here.

Fig. 17 is near here.

Fig. 18 is near here.

Fig. 19 is near here.

Fig. 20 is near here.

Fig. 21 is near here.

Fig. 22 is near here.

The above comparative analysis was only selected to compare the best results after 20 runs, and it was not compared with the classical model. Therefore, in order to reflect the superiority of the model in precipitation prediction, a comparative analysis will be performed with the particle algorithm optimized bp neural network (PSO-BP), support vector machine (SVM) and PSO-CNN, and the average value of the evaluation index of 20 runs will be selected for comparative analyses. **Table 11** and **Table 12** show the magnitudes of the evaluation indicators of the four models after predicting precipitation in Ankang and Yongding, from which it can be seen that the error indicators of VMD-MSMA-LSTM-ARIMA are always the smallest and the NSE indicators tend to be close to 1, proving the superiority of the model in precipitation prediction as well as its high reliability.The superiority of this model can be visualized in **Fig. 23**, and **Fig. 24** is a Taylor diagram of the model, looking to see that VMD-MSMA-LSTM-ARIMA is closest relative to the observation points, representing its high prediction accuracy. **Fig. 25** and **Fig. 26** show the histograms of the error frequency distribution of the four models predicting precipitation in two regions, from which it can be seen that the error of VMD-MSMA-LSTM-ARIMA is roughly distributed in [-4,4], In the error interval of [-4,4], the error percentage of VMD-MSMA-LSTM-ARIMA, PSO-BP, PSO-CNN, SVM predicting precipitation in Ankang precipitation is 57.3%, 7.32%, 13.4%, 14.6% and for Yongding precipitation errors in the interval are 71.3%, 4.66%, 6.97%, 5.83%,which has a small error and conforms to the normal distribution, indicating that the model is more stable, while the error values of the prediction results of the other three models are generally larger. **Fig. 27** shows the box plots of the prediction results of the four models, from which it can be seen that VMD-MSMA-LSTM-ARIMA have super high similarity with the actual values, for example, the highest values of the four models are 216.64, 181,185.37, 136.03, where the present model is more approximate.

Table 11 is near here.

Table 12 is near here.

Fig. 23 is near here.

Fig. 24 is near here.

Fig. 25 is near here.

Fig. 26 is near here.

Fig. 27 is near here.

4.8 Uncertainty analysis

In an uncertainty analysis of different models was also performed in this study. The instability of the models mainly arises due to the uncertainty of the model parameters and the noise of the data. Therefore, we analyzed the uncertainty of eight different machine learning methods using *PICP* as well as *MPI*. The *PICP* and *MPI* values calculated for all parameters in the test dataset are shown in **Table 13**. From the table, it can be seen that the VMD-MSMA-LSTM-ARIMA model has a wider prediction interval than the other models, and it can be seen that the model has the highest *PICP* value, i.e., the number of observations entering the 95% confidence band, than the other models. the VMD-MSMA-LSTM-ARIMA model predicts the precipitation in Ankang (*PICP*=0.98780) with the uncertainty is the lowest and the prediction performance is the most stable. In the precipitation prediction for Yongding district, the VMD-MSMA-LSTM-ARIMA, VMD-MSMA-LSTM, VMD-SMA-LSTM, VMD-WOA-LSTM, VMD-MFO--LSTM, and VMD-LSTM models all have a *PICP* value of 1. The models have a very high degree of prediction certainty, which is better than SMA-LSTM, and LSTM model also has better performance.

Table 13 is near here.

In addition, the mean values after 20 runs were also analyzed for uncertainty, and it can be seen from **Table 14** that VMD-MSMA-LSTM-ARIMA has the highest *PICP* comparison among the four models, and can reach 1 in Yongding precipitation, thus proving once again that the model has accurate predictability and can be applied to precipitation prediction.

Table 14 is near here.

5 Conclusion

In this study, a precipitation prediction model based on VMD-MSMA-LSTM-ARIMA is proposed and used to make short-term predictions of precipitation in Ankang City, Shaanxi Province and Yongding District, Fujian Province, respectively. The model adopts the decomposition-summary design idea, firstly, the monthly precipitation data are decomposed into modal data with different frequencies by VDM, and the overall residuals are calculated, which will be input into the MSMA-LSTM-ARIMA model for prediction respectively, and finally the predicted values of each component are aggregated to obtain the final prediction results of precipitation. The empirical results show that the model can obtain high accuracy of non-stationary precipitation prediction and has good regional adaptability, and the conclusions are as follows:

(1) The VMD decomposition is adopted to achieve a smoother and more stable subsequence, which improves the accuracy of the model prediction. Moreover, the model predicts the nonlinear smooth Residuals as well, which further improves the accuracy.

(2) The ARIMA model has strong fitting ability for linear data, while the LSTM has accurate capturing ability for complex nonlinear series prediction, and the combination of the two complements each other, thus improving the accuracy of the prediction.

(3) The selection of hyperparameters of LSTM has a great influence on the model prediction accuracy. The SMA selected in this project is a swarm intelligence algorithm for optimization with fast convergence speed and strong search capability. Moreover, this paper adopts adaptive and spiral search strategies to strengthen the global finding capability of the sticky bacterium optimization algorithm, which not only can realize automatic parameter adjustment, but also makes the setting of hyperparameters better.

Nevertheless, there are still improvements to the model. First, the proposed model requires separate LSTM-ARIMA models for each decomposed series as well as the residuals, which requires the use of the MSMA algorithm to calibrate the parameters and therefore has a long runtime. The length of the data series is required to better capture the long-term correlation of the series and improve the prediction accuracy. Second, SMA randomly selects two individuals for position and direction updates, which limits its search capability, and SMA has the problem of low

convergence accuracy. Nowadays, new intelligent optimization algorithms are emerging **(Faramarzi, *et al.* 2020; Abualigah, *et al.* 2021)**, and whether the new optimization algorithms can make the model prediction more accurate remains to be studied in comparison. Third, the prediction of residual values was also only roughly performed with the LSTM-ARIMA model prediction, without comparison with other combined models, and whether there are better models for the prediction of residuals needs to be further explored.

In addition, precipitation is a complex dynamic system that is influenced by many external environmental variables and human activities. The VMD-MSMA-LSTM-ARIMA model used in this study is a data-driven study, which ignores the interference of external factors on precipitation prediction, which is one of the inherent shortcomings of the model. Therefore, the introduction of external variables is an important research concern for the next step. We also believe that with the development of deep learning and the deepening understanding of precipitation process, the prediction of future precipitation will also be more accurate, so as to better guide agricultural production and flood prevention and disaster prevention, and promote the harmonious development of human society.

Disclosure statement

No potential conflict of interest was reported by the authors.

Funding

It was supported by the Open Research Fund of State Key Laboratory of Simulation and Regulation of Water Cycle in River Basin, China Institute of Water Resources and Hydropower Research (grant No. IWHR-SKL-201905).

References

Abualigah, L., Diabat, A., Mirjalili, S., Abd Elaziz, M., and Gandomi, A. H., 2021. The arithmetic optimization algorithm. *Computer methods in applied mechanics and engineering*, 376, 113609.

Adikari, K. E., Shrestha, S., Ratnayake, D. T., Budhathoki, A., Mohanasundaram, S., and Dailey, M. N., 2021. Evaluation of artificial intelligence models for flood and drought forecasting in arid and tropical regions. *Environmental Modelling & Software*, 144, 105136.

Al-Sabhan, W., Mulligan, M., and Blackburn, G. A., 2003. A real-time hydrological model for flood prediction using GIS and the WWW. Computers, *Environment and Urban Systems*, 27(1), 9-32.

Alizadeh, Z., Yazdi, J., and Najafi, M. S., 2022. Improving the outputs of regional heavy rainfall forecasting models using an adaptive real-time approach. *Hydrological Sciences Journal*.

Brown, J. D., Seo, D. J., and Du, J., 2012. Verification of precipitation forecasts from NCEP's Short-Range Ensemble Forecast (SREF) system with reference to ensemble streamflow prediction using lumped hydrologic models. *Journal of Hydrometeorology*, 13(3), 808-836.

Carvalho, T. M. N. and de Assis de Souza Filho, F., 2021. Variational mode decomposition hybridized with gradient boost regression for seasonal forecast of residential water demand. *Water Resources Management*, 35(10), 3431-3445.

Dikshit, A. and Pradhan, B., 2021. Explainable AI in drought forecasting. *Machine Learning with Applications*, 6, 100192.

Dion, P., Martel, J. L., and Arsenault, R., 2021. Hydrological ensemble forecasting using a multi-model framework. *Journal of Hydrology*, 600, 126537.

Dragomiretskiy, K. and Zosso, D., 2013. Variational mode decomposition. *IEEE transactions on signal processing*, 62(3), 531-544.

Di Nunno, F., Granata, F., Pham, Q. B., and de Marinis, G., 2022. Precipitation Forecasting in Northern Bangladesh Using a Hybrid Machine Learning Model. *Sustainability*, 14(5), 2663.

Elsanabary, M. H. and Gan, T. Y., 2015. Evaluation of climate anomalies impacts on the Upper Blue Nile Basin in Ethiopia using a distributed and a lumped hydrologic model. *Journal of Hydrology*, 530, 225-240.

Fan, D., Sun, H., Yao, J., Zhang, K., Yan, X., and Sun, Z., 2021. Well production forecasting based on ARIMA-LSTM model considering manual operations. *Energy*, 220, 119708.

Faramarzi, A., Heidarinejad, M., Mirjalili, S., and Gandomi, A. H., 2020. Marine Predators Algorithm: A nature-inspired metaheuristic. *Expert Systems with Applications*, 152, 113377.

Gers, F. A., Eck, D., and Schmidhuber, J., 2002. Applying LSTM to time series predictable through time-window approaches. In Neural Nets WIRN Vietri-01 (pp. 193-200). Springer, London.

Haidar, A. and Verma, B., 2018. Monthly rainfall forecasting using one-dimensional deep

convolutional neural network. *IEEE Access*, 6, 69053-69063.

Houssein, E. H., Mahdy, M. A., Blondin, M. J., Shebl, D., and Mohamed, W. M., 2021. Hybrid slime mould algorithm with adaptive guided differential evolution algorithm for combinatorial and global optimization problems. *Expert Systems with Applications*, 174, 114689.

Ilyés, C., Wendo, V. A., Carpio, Y. F., and Szűcs, P., 2021. Differences and similarities between precipitation patterns of different climates. *Acta Geodaetica et Geophysica*, 56(4), 781-800.

Jalalkamali, A. and Jalalkamali, N., 2011. Groundwater modeling using hybrid of artificial neural network with genetic algorithm. *African Journal of Agricultural Research*, 6(26), 5775-5784.

Kang, J., Wang, H., Yuan, F., Wang, Z., Huang, J., and Qiu, T., 2020. Prediction of precipitation based on recurrent neural networks in Jingdezhen, Jiangxi Province, China. *Atmosphere*, 11(3), 246.

Kumar, D., Singh, A., Samui, P., and Jha, R. K., 2019. Forecasting monthly precipitation using sequential modelling. *Hydrological sciences journal*, 64(6), 690-700.

Li, G., Chang, W., and Yang, H., 2020. A novel combined prediction model for monthly mean precipitation with error correction strategy. *IEEE Access*, 8, 141432-141445.

Li, W., Zhao, S., Chen, Y., Wang, L., Hou, W., Jiang, Y., Zou, X., and Shi, S., 2022. State of China's climate in 2021. *Atmospheric and Oceanic Science Letters*, 100211.

Li, X., Rankin, C., Gangrade, S., Zhao, G., Lander, K., Voisin, N., Shao, M., Morales-Hernández, M., Kao, S., and Gao, H., 2021. Evaluating precipitation, streamflow, and inundation forecasting skills during extreme weather events: A case study for an urban watershed. *Journal of Hydrology*, 603, 127126.

Liang, Z., Xiao, Z., Wang, J., Sun, L., Li, B., Hu, Y., and Wu, Y., 2019. An improved chaos similarity model for hydrological forecasting. *Journal of Hydrology*, 577, 123953.

Lin, K., Lin, J., and Chen, B., 2008. Study on short-range precipitation forecasting method based on genetic algorithm neural network. In 2008 7th World Congress on Intelligent Control and Automation. *IEEE*, 7883-7887.

~~Long, Y., He, X. G., and Zhang, X. P., 2015. Particle Swarm Optimized Wavelet Neural Network Models for Forecasting Monthly Precipitation. *Computer Science*.~~

Mahavarpour, Z., 2014. The Analysise of Occurrences Daily Precipitation Probability in Iran and Forecast by Using Markov Chain Model. *Geographical Research*, 29(4), 239-251.

Nickerson, D. M. and Madsen, B. C., 2005. Nonlinear regression and ARIMA models for precipitation chemistry in East Central Florida from 1978 to 1997. *Environmental Pollution*, 135(3), 371-379.

Papacharalampous, G., Tyralis, H., and Koutsoyiannis, D., 2018. Predictability of monthly temperature and precipitation using automatic time series forecasting methods. *Acta Geophysica*, 66(4), 807-831.

Pradhan, N. S., Fu, Y., Zhang, L., and Yang, Y., 2017. Farmers' perception of effective drought policy implementation: A case study of 2009–2010 drought in Yunnan province, China. *Land use policy*, 67, 48-56.

Samantaray, S. and Sahoo, A., 2021. Prediction of suspended sediment concentration using hybrid SVM-WOA approaches. *Geocarto International*, 1-27.

Seo, S. B. and Sung, J. H., 2020. The role of probabilistic precipitation forecasts in hydrologic predictability. *Theoretical and Applied Climatology*, 141(3), 1203-1218.

Siddique, R., Mejia, A., Brown, J., Reed, S., and Ahnert, P., 2015. Verification of precipitation forecasts from two numerical weather prediction models in the Middle Atlantic Region of the USA: A precursory analysis to hydrologic forecasting. *Journal of Hydrology*, 529, 1390-1406.

Simon, T., Fabsic, P., Mayr, G. J., Umlauf, N., and Zeileis, A., 2018. Probabilistic forecasting of thunderstorms in the Eastern Alps. *Monthly Weather Review*, 146(9), 2999-3009.

Sun, X., Qiao, S. F., and Xie, J. R., 2014. The study of precipitation forecast model on EMD-RBF neural network-a case study on northeast china. *Applied Mechanics and Materials*, 641, 119-122.

Tang, A. D., Tang, S. Q., Han, T., Zhou, H., and Xie, L., 2021. A Modified Slime Mould Algorithm for Global Optimization. *Computational Intelligence and Neuroscience*, 2021, 1-22.

~~Tong, Liu, X. H., Yang, Q. R., Xue, F., and Song. (2019). Application of Weighted Markov Chain in Precipitation Forecast in Beijing. DEStech Publications.~~

Toufani, P., Fakheri Fard, A., Mosaedi, A., and Dehghani, A., 2015. Prediction of precipitation applying Wavelet and ANN Model. *Journal of Range and Watershed Managment*, 68(3), 553-571.

Van der Plas, E., Schmeits, M., Hooijman, N., and Kok, K., 2017. A comparative verification of high-resolution precipitation forecasts using model output statistics. *Monthly Weather Review*,

145(10), 4037-4054.

Van Straaten, C., Whan, K., and Schmeits, M., 2018. Statistical postprocessing and multivariate structuring of high-resolution ensemble precipitation forecasts. *Journal of Hydrometeorology*, 19(11), 1815-1833.

Wang, X., Wang, Y., Yuan, P., Wang, L., and Cheng, D., 2021. An adaptive daily runoff forecast model using VMD-LSTM-PSO hybrid approach. *Hydrological Sciences Journal*, 66(9), 1488-1502.

Whan, K. and Schmeits, M., 2018. Comparing area probability forecasts of (extreme) local precipitation using parametric and machine learning statistical postprocessing methods. *Monthly Weather Review*, 146(11), 3651-3673.

Wu, H., Li, X., Schumann, G. J. P., Alfieri, L., Chen, Y., Xu, H., Wu, Z., Lu, H., Hu, Y., Zhu, Q., Huang, Z., Chen, W., and Hu, Y., 2021. From China's heavy precipitation in 2020 to a "Glocal" hydrometeorological solution for flood risk prediction. *Advances In Atmospheric Sciences*, 38(1), 1-7.

Wu, J. and Wang, Z., 2022. A hybrid model for water quality prediction based on an artificial neural network, wavelet transform, and long short-term memory. *Water*, 14(4), 610.

Yang, C., Yuan, H., and Su, X., 2020. Bias correction of ensemble precipitation forecasts in the improvement of summer streamflow prediction skill. *Journal of Hydrology*, 588, 124955.

Yang, H., Liu, S., and Zhang, H., 2017. Adaptive estimation of VMD modes number based on cross correlation coefficient. *Journal of Vibroengineering*, 19(2), 1185-1196.

Yazdandoost, F., Zakipour, M., and Izadi, A., 2021. Copula based post-processing for improving the NMME precipitation forecasts. *Heliyon*, 7(9), e07877.

Zeng, J., Li, J., Lu, X., Wei, Z., Shangguan, W., Zhang, S., Dai, Y., and Zhang, S., 2022. Assessment of global meteorological, hydrological and agricultural drought under future warming based on CMIP6. *Atmospheric and Oceanic Science Letters*, 15(1), 100143.

Zhang, H., Loáiciga, H. A., Ren, F., Du, Q., and Ha, D., 2020. Semi-empirical prediction method for monthly precipitation prediction based on environmental factors and comparison with stochastic and machine learning models. *Hydrological Sciences Journal*, 65(11), 1928-1942.

Zhang, J., Xiao, H., and Fang, H., 2022. Component-based Reconstruction Prediction of Runoff at Multi-time Scales in the Source Area of the Yellow River Based on the ARMA Model. *Water*

Resources Management, 36, 1-16.

Zhang, Z. C., Zeng, X. M., Li, G., Lu, B., Xiao, M. Z., and Wang, B. Z., 2022. Summer Precipitation Forecast Using an Optimized Artificial Neural Network with a Genetic Algorithm for Yangtze-Huaihe River Basin, China. *Atmosphere*, 13(6), 929.

四、专利（著作权）

1. 授予专利（著作权）统计表

序号	作者姓名	专利名称/著作权名称	专利/著作权类型	获批的专利号/授权号
1	魏仁杰；苑晓聪;陈成明;徐信;姜子昂	输料桶（水产养殖）	外观设计专利	ZL202230608028.9
2	苑晓聪,魏仁杰;崔秀芳;陈成明;徐信;姜子昂	垃圾收集航行器（水产养殖）	外观设计专利证书	ZL202230611811.0
3	徐伟铃；丁卫宏;邱明	电气数字化运维服务系统	计算机软件	2023SR0546526

2. 专利（著作权）证书汇编

证书号第7975298号

外观设计专利证书

外观设计名称：输料桶（水产养殖）

设　计　人：魏仁杰;苑晓聪;陈成明;徐信;姜子昂

专　利　号：ZL 2022 3 0608028.9

专利申请日：2022年09月15日

专利权人：上海海洋大学

地　　址：201306 上海市浦东新区沪城环路999号

授权公告日：2023年04月07日　　授权公告号：CN 307957784 S

国家知识产权局依照中华人民共和国专利法经过初步审查，决定授予专利权，颁发外观设计专利证书并在专利登记簿上予以登记。专利权自授权公告之日起生效。专利权期限为十五年，自申请日起算。

专利证书记载专利权登记时的法律状况。专利权的转移、质押、无效、终止、恢复和专利权人的姓名或名称、国籍、地址变更等事项记载在专利登记簿上。

局长
申长雨

国家知识产权局
2023年04月07日

第 1 页 (共 2 页)

证书号第7761353号

外观设计专利证书

外观设计名称：垃圾收集航行器（水产养殖）

设　计　人：苑晓聪;魏仁杰;崔秀芳;陈成明;徐信;姜子昂

专　利　号：ZL 2022 3 0611811.0

专利申请日：2022 年 09 月 16 日

专 利 权 人：上海海洋大学

地　　址：201306 上海市浦东新区沪城环路 999 号

授权公告日：2022 年 12 月 20 日　　授权公告号：CN 307739312 S

国家知识产权局依照中华人民共和国专利法经过初步审查，决定授予专利权，颁发外观设计专利证书并在专利登记簿上予以登记。专利权自授权公告之日起生效。专利权期限为十五年，自申请日起算。

专利证书记载专利权登记时的法律状况。专利权的转移、质押、无效、终止、恢复和专利权人的姓名或名称、国籍、地址变更等事项记载在专利登记簿上。

局长
申长雨

国家知识产权局
2022年12月20日

第 1 页（共 2 页）

其他事项参见续页

中华人民共和国国家版权局

计算机软件著作权登记证书

证书号： 软著登字第11133697号

软 件 名 称： 电气数字化运维服务系统 V1.0

著 作 权 人： 徐伟钤;丁卫宏;邱玥

开发完成日期： 2023年04月06日

首次发表日期： 2023年04月07日

权利取得方式： 原始取得

权 利 范 围： 全部权利

登 记 号： 2023SR0546526

根据《计算机软件保护条例》和《计算机软件著作权登记办法》的规定，经中国版权保护中心审核，对以上事项予以登记。

中华人民共和国国家版权局 计算机软件著作权登记专用章

No. 12636171

2023年05月17日